# Peak detection in sediment-charcoal records: impacts of alternative data analysis methods on fire-history interpretations

Philip E. Higuera[1*], Daniel G. Gavin[2], Patrick J. Bartlein[2], Douglas J. Hallett[3,4]

1. Department of Forest Ecology and Biogeoscience, University of Idaho, Moscow ID 83844, USA

2. Department of Geography, University of Oregon, Eugene OR 97493, USA

3. Biogeoscience Institute, University of Calgary, Calgary, Alberta, T2N 1N4, Canada

4. School of Environmental Studies, Queen's University, Kingston, Ontario, K7L 3N6, Canada

* corresponding author

Running head: Fire history from sediment charcoal records

Additional key words: paleoecology, bias, sensitivity, charcoal analysis

**Summary (50 words):**

Charcoal peaks in lake sediments provide valuable records of fire history in stand-replacing fire regimes. Despite increasing use of this proxy, data analysis methods vary and have not been systematically compared. We demonstrate important biases between methods and make recommendations based on analyses of simulated and empirical datasets.

**Abstract**

Over the past several decades high-resolution sediment-charcoal records have been increasingly used to reconstruct local fire history. Data analysis methods usually involve a decomposition that detrends a charcoal series and then applies a threshold value to isolate individual peaks which are interpreted as fire episodes. Despite the proliferation of these studies, methods have evolved largely in the absence of a thorough statistical framework. We describe eight alternative decomposition models (four detrending methods used with two threshold-determination methods) and evaluate their sensitivity to a set of known parameters integrated into simulated charcoal records. Results indicate that the combination of a globally-defined threshold with specific detrending methods can produce strongly biased results, depending on whether or not variance in a charcoal record is stationary through time. These biases are largely eliminated by using a locally-defined threshold, which adapts to changes in variability throughout a charcoal record. Applying the alternative decomposition methods on three previously-published charcoal records largely supports our conclusions from simulated records. We also present a minimum-count test for empirical records, which reduces the likelihood of false positives

when charcoal counts are low. We conclude by discussing how to evaluate when peak detection methods are warranted with a given sediment record.

## Introduction

High-resolution charcoal records are an increasingly common source of fire-history information, particularly in ecosystems where tree-ring records are short relative to average fire-return intervals (Gavin *et al.* 2007). Over the past several decades numerous studies have used peaks in charcoal accumulation in sediment records to estimate the timing of "fire episodes", one or more fires within the sampling resolution of the sediment record (Whitlock and Larsen 2001). Identifying fire episodes from charcoal records is most promising when fires are (1) large, (2) burn with high severity, and (3) recur with average intervals at least five times the sampling resolution of the sediment record (Clark 1988b, Whitlock and Larsen 2001, Higuera *et al.* 2005, Higuera *et al.* 2007). Sediment-charcoal records are thus particularly valuable for studying stand-replacing fire regimes in boreal and subalpine forests, where all three of these conditions are typically met.

Interpreting fire episodes from sediment-charcoal records would be straightforward if they were characterized by low levels of charcoal punctuated by unambiguous peaks. In reality, however, charcoal records are complex and non-stationary, i.e., their mean and/or variance change over time (Clark *et al.* 1996, Clark and Patterson 1997, Long *et al.* 1998). Empirical and theoretical studies (e.g., Marlon *et al.* 2006, Higuera *et al.* 2007) suggest that non-stationarity in charcoal records can arise from at least two sets of processes: (1) changes in the fire regime including the rate of burning,

the intensity of fires, the type of vegetation burned, and thus charcoal production per unit time, and/or (2) changes in the efficiency of charcoal delivery to the lake center (taphonomy) due to changing rates of slope wash and/or within-lake redeposition. The latter process, known as sediment focusing, can greatly affect the sediment accumulation rate as a lake infills (Davis *et al.* 1984, Giesecke and Fontana 2009) and may produce long-term trends in charcoal records unrelated to changes in the fire regime. Recognizing the importance of these processes, paleoecologists have applied a range of statistical methods to charcoal data in order to isolate the signal related to "local" fire occurrence (e.g., within 0.5-1.0 km; Gavin *et al.* 2003, Lynch *et al.* 2004a, Higuera *et al.* 2007) and reconstruct fire history. Despite the proliferation of statistical methods for peak identification, seemingly no study has discussed the assumptions underlying alternative methods and their impacts on fire-history interpretations.

Here we address several key issues related to peak identification in high-resolution, macroscopic charcoal records[1] by using simulated and empirical charcoal records. We start by discussing some important statistical properties of macroscopic charcoal records and then describe the motivation for statistical treatments. We briefly review how different methods have been applied, and then introduce a typology of methods, including their respective assumptions and justifications. Second, we illustrate and quantify the biases that these techniques can introduce to fire-history interpretations by applying them to simulated charcoal records. Third, we apply the same methods to three previously-published charcoal records from conifer forests to demonstrate potential

[1] We refer to macroscopic charcoal records as those quantifying charcoal not passing through a sieve of 125 μm or larger.

biases in empirical records, and we introduce a technique to minimize some of these biases. Finally, we conclude with recommendations of specific methodologies and a discussion of how analysts can evaluate the suitability of records for peak identification rather than other qualitative or quantitative analyses.

## Temporal variability in charcoal time series

Charcoal time series can be generally characterized as "noisy", and they contain many forms of non-stationarity, including changing short-term variability superimposed on a slowly varying mean (Long *et al.* 1998, Higuera *et al.* 2007). Changes in variability, or *heteroscedasticity*, have implications for the particular goal of data analysis. When the goal is to quantify changes in total charcoal input, as an index of biomass burning for example, heteroscedasticity violates the assumptions of parametric statistics useful in this context, e.g., analysis of variance and regression. In particular, in analysis of variance (or in the t-test of the difference of means in the case of two periods) heteroscedasticity increases the probability of Type I error, falsely inferring significant differences between periods (Underwood 1997). Similarly, in regression analysis fitting a trend line to charcoal data with changing variability over time can increase the variability of the slope coefficient. Changes in variability (besides being interesting in their own right) can thus lead to false conclusions about the significance of long-term trends or differences between different parts of a record. In practice, heteroscedasticity is usually dealt with by applying a "variance-stabilizing transformation" (Emerson 1983) that acts to homogenize variance across a record. As will be illustrated below, when the goal of charcoal analysis is peak identification, transformation can lead to the exaggeration of some peaks and

suppression of others. Consequently, the specific approach taken (whether to transform or not), should depend upon the overall focus of an analysis. In this paper we focus on the goal of detecting local fires through peak detection.

**Analytical methods for inferring local fire occurrence**

Following Clark's pioneering work (1988b, 1990) in which fire events surrounding small lakes were identified from charcoal in thin-sections of laminated sediments, similar approaches were developed for quantifying macroscopic charcoal abundance and subsequently adopted by a large number of research groups (Table 1; See also Whitlock and Larsen 2001). Most techniques quantify charcoal as either the total number of pieces or surface area ($mm^2$) of charcoal in a particular size class, within volumetric subsamples taken contiguously through sediment cores (typically at 0.5 to 1.0 cm resolution, corresponding to ca. 10-25 year resolution for most lakes). The resulting concentration of charcoal (pieces $cm^{-3}$, or $mm^{-2}$ $cm^{-3}$) in each level is multiplied by the estimated sediment accumulation rate (cm $yr^{-1}$) to obtain the charcoal accumulation rate (CHAR, pieces $cm^{-2}$ $yr^{-1}$ or $mm^{-2}$ $cm^{-2}$ $yr^{-1}$). Sediment accumulation rates, and the age of each sample, are estimated by an age-depth model based on radiometric dates, tephra layers, and any additional sources of age information. The use of accumulation rates can potentially correct for changing sediment accumulation rates that would dilute or concentrate charcoal in a given volume of sediment, and as mentioned above, may also be affected by sediment focusing processes. Usually, the CHAR series is interpolated to a constant temporal resolution to account for unequal sampling intervals resulting from variable sediment accumulation rates. This step is necessary to develop threshold

statistics that are not biased to a particular portion of a record, and to standardized within- and between-site comparisons.[2] Hereafter we refer to the interpolated CHAR series as *C*. The analytical choices and sources of error in the development of a charcoal record are briefly summarized in Table 2 and discussed in detail by Whitlock and Larsen (2001).

At this point, most *C* series can be characterized as an irregular time series with discrete peaks superimposed on a slowly varying mean. While the size of any individual peak reflects the size, location, and charcoal production of individual fires, the average size of peaks may change through time, contributing to a slowly changing variance. This non-stationarity may arise, as discussed above, due to variations in charcoal production per unit time and/or variable taphonomic and sedimentation processes. Without knowledge of whether non-stationarity is due to changes in taphonomy and sedimentation or to real changes in fire history, it is reasonable to stabilize the variance of peak heights so as to not "pass over" periods of low charcoal. This motivates the manipulation of *C* to produce a stationary series in which all local fires would theoretically result in similar range of peak sizes. Doing so would allow for the application of a single global threshold value to the final series to separate fire-related from non-fire related peaks.

In practice, determining the size of peaks that represents local fires involves a three-step "decomposition" of the *C* series (Clark *et al.* 1996, Long *et al.* 1998; Fig. 1). First, the slowly-varying mean, or "background" component, $C_{back}$, is modeled through a curve-fitting algorithm, e.g., a locally-weighted regression that is robust to outliers (e.g., Cleveland 1979). The window size for this smoothing varies between studies but is

[2] When sampling intervals are not standardized within a record or between two records, then biases may be introduced when applying criteria uniformly. Interpolation helps minimize, but not remove, this bias, as noted in the last section of this paper.

typically between 100 and 1000 years. Background estimation may be preceded by transforming $C$ (e.g., logarithmically). Second, the background trend is removed from the series by subtraction ($C$-$C_{back}$) or division ($C$/ $C_{back}$), creating a series of residuals or indices, respectively. This detrended series is frequently termed the "peak component," but in the case of indices, it is dimensionless rather than a portion of $C$, as implied by "peak component." Here we use the term "peak series" and notation $C_{peak}$ to refer to the detrended series. Third, a threshold is applied to $C_{peak}$ to separate variability related to local fire occurrence from variability unrelated to local fire occurrence (e.g., random variability and sediment mixing). Peaks exceeding the threshold are the basis for fire frequency and fire return interval calculations.

Here, we present a typology of four possible decomposition approaches based on whether the raw or transformed $C$ series is used and whether $C_{peak}$ is calculated as residuals or index values relative to $C_{back}$ (See Table 3 for abbreviations). The *no-transform-residual model* (NR model hereafter) is a simple subtraction: $C - C_{back}$. The *no-transform-index model* (NI model) is a ratio: $C$ / $C_{back}$. Because background charcoal is in the denominator, the NI model cannot be applied when background charcoal equals zero, which occurs in non-forested or treeline ecosystems (e.g., Huber *et al.* 2004, Higuera *et al.* 2009, Hallett and Anderson 2010). The *transform-residual model* (TR model) first log-transforms $C$ (after adding 1 to guard against negative values) before calculating the background: $\log(C+1) - C_{back}$, where $C_{back} = f(\log(C+1))$ . Finally, the *transform-index* model (TI model) is the ratio of the log-transformed series: $\log(C+1)$ / $C_{back}$, where $C_{back} = f(\log(C+1))$.

Nearly all studies have used the NR or the TI model in charcoal peak analyses (Table 1), but there has been no discussion of the assumptions underlying each model. The NR model implicitly assumes that charcoal peaks from local fires are created through additive processes. That is, charcoal introduced from a fire is added to the total amount of background charcoal (i.e., charcoal delivery to the core site during periods without local fires). Background charcoal may change as redeposition processes change (e.g., wind-mixing of littoral sediment, higher fire frequencies), but the total amount of charcoal produced per fire remains unchanged. Variance stabilization is the goal of the NI, TR, and TI models, which implicitly assume that charcoal peaks from local fires are created through multiplicative processes; i.e., the total amount of charcoal introduced from a local fire is some multiple of background charcoal. Similar variance-stabilization goals used in dendrochronology are typically based on the NI or TR models, rather than the methods more recently adopted for charcoal records (NR and TI models; Table 1). As in dendrochronology (Cook and Peters 1997, Fowler 2009) the choice of detrending model has an important impact on the resulting detrended series.

In comparison with the little attention given to alternative detrending models, recent papers have more carefully addressed the task of determining threshold values for peak identification. Comparison of peaks with known fire events (dated from historical records or tree-rings) may help in selecting a threshold, but historical records often represents only a fraction of a charcoal record, and a wide range of thresholds may still be appropriate (e.g., Gavin *et al.* 2006). Clark *et al.* (1996) addressed this issue by using a sensitivity analysis to test of the number of peaks as a function of changing threshold values. They reasoned that if $C_{peak}$ was comprised of a population of small values (e.g.,

background charcoal) and a smaller population of large values (local fires), then the sensitivity test should detect the split between these populations. Gavin *et al.* (2006) built on this sensitivity test by modeling $C_{peak}$ as a mixture of two Gaussian distributions with different means, variances, and proportional contribution to the total population. The lower distribution is assumed to represent the majority of time during which *C* is small and is affected mainly by distant fires, redeposition, mixing, and random variability; i.e., the "noise" unrelated to specific fires. The upper distribution, ideally distinct from the lower distribution, describes the variability due to local fires and can be considered the "signal" of interest. Gavin *et al.* (2006) suggested that the threshold be at the upper end of the noise distribution, and Higuera *et al.* (2008) further specified that the threshold be at the $95^{th}$, $99^{th}$, or $99.9^{th}$ percentile of the noise distribution. If the noise and signal distributions are distinct, then the variance of the signal distribution ($\sigma^2_S$) would be much larger than that of the noise distribution ($\sigma^2_N$). A signal-to-noise index (SNI; Higuera *et al.* 2009), calculated as $\sigma^2_S/(\sigma^2_S+\sigma^2_N)$ approaches one when the noise distribution is tightly defined with a narrow standard deviation. SNI values less than ≈ 0.5 suggest poor separation of large peaks from the noise-attributable variation. We note these details here because the Gaussian mixture approach assumes that the distribution of $C_{peak}$ values is right-skewed, and therefore variance-stabilizing expressions of $C_{peak}$ (all but the NR model) work against defining a distinct noise distribution.

Unless variance of $C_{peak}$ does not change through time (i.e., it is homoscedastic), selecting a threshold based on the entire series could lead to systematic biases towards detecting small or large peaks (depending on which size dominates the record). While variance-stabilization approaches were developed to address this issue, Higuera *et al.*

(2008a, 2009) introduced a new approach intended to be more adaptable by applying the Gaussian mixture model introduced by Gavin *et al.* (2006) to a 500-year moving window of $C_{peak}$ centered on each time step in the series. This technique is termed a "local threshold," and it accounts for potentially changing variance of $C_{peak}$ by selecting a threshold based on $\sigma^2_N$ in a user-defined subsection of the record. Using smaller sample sizes to compute the Gaussian mixture distribution increases the chance of erratic model fits in a portion of the cases. Thus, it is important to smooth the local thresholds (typically to the same frequency as that use to define $C_{back}$) such that it varies smoothly over time and be cognizant of the total number of samples in each local population (a minimum of ca. 30 is recommended; Higuera *et al.* 2009). This decomposition approach is similar to peak-detection methods in other applications (e.g., Mudelsee 2006) in that it accounts for changes in both the central tendency and variability in a series.

Last, Gavin *et al.* (2006) introduced a test to screen peaks detected by a threshold but may nevertheless result from statistically-insignificant changes in charcoal abundance. This "minimum-count test" applies specifically to studies quantifying charcoal through numbers, as opposed to area, and it examines the possibility that the differences in counts between two samples may result simply from sampling effects. If charcoal count and volume data are available, then it is possible to assess the minimum increase in charcoal count required to be statistically greater than a previous sample, assuming measured counts are Poisson-distributed around the "true" (unknown) count for a given sample volume. The probability that two sample counts, $X_1$ and $X_2$, from sediment volumes, $V_1$ and $V_2$, may originate from the same Poisson distribution is estimated from the *d* statistic:

$$d = \frac{\left| X_1 - (X_1 + X_2)\left(\frac{V_1}{V_1 + V_2}\right)\right| - 0.5}{\sqrt{(X_1 + X_2)\left(\frac{V_1}{V_1 + V_2}\right)\left(\frac{V_2}{V_1 + V_2}\right)}} \quad (1)$$

where the significance of $d$ is assessed from the cumulative normal distribution (Detre and White 1970, Shiue and Bain 1982). This test does not incorporate additional errors in counts from laboratory error (Table 2), and so significance thresholds higher than 0.05 may be warranted. We incorporate the minimum-count test here because the possibility of sampling-related errors increases with the variance-stabilization models (NI, TR, TI) due to the inflation of very small changes in $C$ at times when $C_{back}$ is small (Cook and Peters 1997).

## Methods

To illustrate how analytical choices impact peak identification, we applied the methods introduced above to simulated and empirical charcoal records. With simulated records, where the underlying processes creating a charcoal record are known, we evaluated the sensitivity of each of the four decomposition and the two threshold-determination methods (global and local thresholds) to two hypothetical scenarios (described below). We analyzed the empirical records in the same manner but also applied the minimum-count test to illustrate the impacts of this technique.

### *Simulated Records*

Simulated charcoal records were generated from statistical distributions to reflect two scenarios for the relationship between $C$ and $C_{back}$. In both scenarios, the rate of peak

occurrence (implicitly representing local fires) was constant, but $C_{back}$ increased half-way through the 10,000-yr record. In Scenario 1, charcoal peak heights had a constant variance that was independent of $C_{back}$, representing the assumption that charcoal from local fires is added to a charcoal record through additive processes; thus variability is stationary throughout the record. In Scenario 2, peak heights varied in direct proportion to $C_{back}$, representing a multiplicative relationships between charcoal from local fires and $C_{back}$; thus the charcoal series is heteroscedastic.

Simulated records with 20-yr time steps, $x(i)$, $i$ = 0, 20, 40…10,000, were constructed in three steps, and we use the notation $C_b$ and $C_p$ to refer to the known populations of background and peak charcoal respectively, where as the estimated populations are referred to with $C_{back}$ and $C_{peak}$, as introduced above. First, background charcoal, $C_b$, was prescribed as constant values that increased from a minimum of 50 to a maximum of 100 pieces per 5 $cm^{-3}$ between 5500 and 4500 simulated yr BP. Specifically, the concentration of background charcoal in any 20-yr sample, $x(i)$, was defined as:

$$C_b(i) = \frac{\min(C_b) + \max(C_b)}{1 + \exp[-lrx(i)]} \quad (2)$$

where $l$ = 45 and $r$ = 0.009 and determine the location (in time) and rate of change in $C_b$, respectively. Second, a charcoal series characterized by right-skewed high-frequency variation, $C_p$ (pieces 5 $cm^{-3}$) was calculated from random numbers using a power function, as follows:

$$C_p(i) = b[-\log \varepsilon(i)]^c \quad (3)$$

where $b$ = 35 and determines the location of the distribution, $c$ = 1.25 and creates a distribution slightly more skewed than a log-normal distribution (as found in many empirical records; Marlon *et al.* 2009), and $\varepsilon(i) \approx N(0; 1)$, a random number from a normal distribution with mean 0 and standard deviation 1. Third, the background and peak series (pieces $cm^{-3}$) were added, and then multiplied by the sediment accumulation rate, $s_{acc}$ (cm $yr^{-1}$), to obtain the final series of charcoal accumulation rates (CHAR, pieces $cm^{-2}$ $yr^{-1}$), $C$. For Scenario 1, no further treatment was performed, and:

$$C(i) = s_{acc}[C_b(i) + C_p(i)] \quad (4)$$

For Scenario 2, the $C$ was scaled to background charcoal, $C_b$, as follows:

$$C(i) = s_{acc}\left[\frac{C_b(i)}{\max(C_b)}C_b(i) + C_p(i)\right] \quad (5)$$

As a result, peak heights in Scenario 2 increased proportional to $C_b$, and the structure of the variance changed through the time series.

*Empirical Records*

We selected three high-resolution charcoal records with differing variability in background charcoal and peak heights. Little Lake (Long *et al.* 1998) is located in Douglas-fir forest in the Oregon Coast Range. The 3.3-ha, 4.0-m deep lake is surrounded by a fen and has a small inflowing stream draining a 597-ha watershed (Marlon *et al.* 2006; C. Long, personal communication, November 2009). The 11.3-meter core has overall $C$ values similar to the simulated records (median = 14.4 pieces $cm^{-2}$ $yr^{-1}$). Over

its 9000-yr record $C_{back}$ varies between 0.94 and 44.04 pieces $cm^{-2}$ $yr^{-1}$, and vegetation was consistently dominated by Douglas-fir. Rockslide Lake (Gavin *et al.* 2006) is located in subalpine forest in southeast British Columbia. The 3.2-ha, 14.1-m deep lake is fed by an intermittent stream within an 86-ha watershed. The 2.1-m core has overall *C* values lower than Little Lake (median = 0.49 pieces $cm^{-2}$ $yr^{-1}$). Over its 5000-year record $C_{back}$ varies between 0.06 and 1.13 pieces $cm^{-2}$ $yr^{-1}$, and vegetation was consistently dominated by Engelmann spruce and subalpine fir. Finally, Ruppert Lake (Higuera *et al.* 2009) is located in boreal forest of Alaska's south-central Brooks Range. The 3-ha, 7.0-m deep lake has a ca. 200-ha watershed with subdued topography and a small inflowing stream. The 4.8-m core has the lowest overall *C* values of all three records (median = 0.04 pieces $cm^{-2}$ $yr^{-1}$). Over the 14,000-year record $C_{back}$ ranges from 0.00-0.22 pieces $cm^{-2}$ $yr^{-1}$ with a distinct increase around 5000 yr, coincident with the transition from a forest-tundra to boreal forest vegetation. Overall, five different vegetation types dominated the landscape around Ruppert Lake during the record.

For all records, we used the published age-depth relationship but reanalyzed each series using the published resampling intervals of 10, 10, and 15 yr for Little, Rockslide, and Ruppert lakes, respectively. We did not use the same analysis parameters as in the published records, since our purpose was to test different parameters. We calculated background charcoal using a locally weighted regression robust to outliers (lowess) in a 500-year window. The robust lowess model is less sensitive to non-stationarity and thus may be applied to raw and transformed data (Cleveland 1979).

Data transformation, peak identification, and sensitivity analysis

We applied the four different detrending models to each simulated and empirical record, and we used a modified Levene's test of equal variance (based on sample medians; Brown and Forsythe 1974) to test the null hypothesis of equal variance between two portions of each record. Sample sizes for p-value calculations were adjusted to account for temporal autocorrelation in each record following Bretherton *et al.* (1999). For simulated records, we compared the periods 10,000-6000 and 4000-0 yr BP. We present only the median test result for 500 realizations of the simulated series.[3] For empirical records we subjectively selected periods where background charcoal had two qualitatively different levels and then divided this period in half for comparison. At Little, Rockslide, and Ruppert lakes, these periods corresponded to the last 8000, 5000, and 10,000 years, respectively. The test statistic, $W_{50}$, is used as an index of heteroscedasticity, and the associated p-value is used to assess the null hypothesis of equal variance.

We identified peaks in simulated and empirical records using a Gaussian mixture model that models the noise distribution within $C_{peak}$ (described earlier). In this application, the value of the mixture model is its ability to apply uniform treatments to all records, making specific threshold-selection parameters of less importance. For all analyses, we used the 99$^{th}$ percentile of the modeled noise distribution as the threshold

[3] Results did not differ when analyzing 250, 500, or 1000 realizations (each 10,000 yr long), suggesting that the inherent variability captured.

value.[4] Thresholds were defined both globally (a single mixture model fit to the entire record) or locally (fitting the mixture models to 500-year windows centered on each sample, and then smoothing the series of resulting threshold values).

For the simulated records, we quantified the sensitivity of peak identification to the four detrending models with a sensitivity ratio, *s*. We defined *s* as the number of peaks detected in the first half of each record divided by the total number of peaks detected in the second half of each record. If an analytical method is insensitive to variations in $C_{back}$, then *s* will equal one. Values of *s* significantly greater or less than one indicate a systematic bias in the set of analytical methods. We used a Monte Carlo approach to estimate the value of *s* for each of the 16 analysis combinations (2 simulation scenarios x 4 detrending models x 2 threshold-determination techniques = 16). For each combination, *s* was estimated by the average *s* from 500 simulations, and the 2.5$^{th}$ and 97.5$^{th}$ percentiles were used to estimate 95% confidence intervals around *s*. If the 95% confidence intervals overlapped one, then the ratio was considered no different from one and the method was deemed insensitive to the variation in background charcoal.

We performed two additional analyses on the empirical records. First, we explored the effect of the four detrending models on the capacity of the Gaussian mixture model to identify a distinct noise distribution. For simplicity, we chose to use only a globally-fit model applied to the Rockslide Lake record, the least variable record; similar examples could be based on subsections of other records. As a metric of how distinct peaks were from $C_{back}$, we examined the SNI (defined earlier) of the fitted Gaussian

[4] Note that the exact threshold criterion used here has no consequence on our interpretations, because interpretations are based on relative changes across a record. For example, analysis using the 95$^{th}$ percentile produced identical patterns.

mixture model. Second, to illustrate the impact of the eight alternative decomposition methods and the minimum-counts test, we applied each method to the empirical records. We quantified the percent of peaks that fail to pass the minimum count test under each decomposition method, and to illustrate how interpretations may differ, we summarized peaks (after removing those failing to pass the minimum-count test) with 1000-yr smoothed peak frequency curves (peaks 1000-yr$^{-1}$, smoothed to 1000 yr with a lowess filter).

## Results

### *Simulated Records*

As designed, simulated charcoal records from Scenario 1 were homoscedastic (500-sample median $W_{50}$ = 0.45, median p = 0.502), while records from Scenario 2 were heteroscedastic ($W_{50}$ = 21.87, p < 0.001; Table 4, Fig. 2). For both scenarios, the choice of decomposition method had a major effect on the variability in the resulting peak series, $C_{peak}$ (Table 4, Fig. 2). Under Scenario 1, only the NR model resulted in a stationary series ($W_{50}$ = 0.44, p = 0.508; Fig. 2; Table 4). The TR and NI models greatly inflated variance when background charcoal was low ($W_{50}$ = 46.72, 25.62; p $\leq$ 0.001), and the TI model further inflated variance ($W_{50}$ = 98.54; p < 0.001). No model stabilized variance in records from Scenario 2 (Table 4, Fig. 2). The NR model preserved heteroscedasticity in the original record ($W_{50}$ = 21.81), the TR and NI models reduced heteroscedasticity ($W_{50}$ = 7.12, 10.81), while the TI model increased heteroscedasticity ($W_{50}$ = 57.92). The skewness of $C_{peak}$ also varied greatly among models. For both Scenario 1 and Scenario 2, the NI model produced the most skewed peak series (3.47 and 3.03), followed closely by

the NR model (2.59, 2.97), and the TI (1.21, 1.55) and TR (0.95, 1.20) models (Table 4, Fig. 2).

In simulated records, threshold type was more important than detrending model when evaluating the sensitivity of peak identification to changes in variance (Fig. 3). Locally-defined thresholds were insensitive to the presence of heteroscedasticity (Scenario 2 vs. Scenario 1) and detrending model (*s* for all scenarios did not differ from 1). In contrast, using a globally-defined threshold produced unbiased results only under three conditions. When *C* was characterized by constant variance (Scenario 1), a globally-defined threshold was unbiased when $C_{peak}$ was defined by residuals: median *s* for NR and TR models was 1.00 (95% CI 0.76-1.33) and 1.17 (0.92-1.54), respectively. Using an index to define $C_{peak}$ inflated variance when $C_{back}$ was low (Fig. 2), resulting in 1.86-2.55 times the number of detected peaks: *s* for NI and TI models was 1.86 (1.24-3.00) and 2.55 (1.50-4.56), respectively. When variance in *C* increased with $C_{back}$ (Scenario 2), transforming *C* and using residuals produced unbiased results, as did creating an index from the non-transformed series: *s* for TR and NI models was 0.85 (0.63-1.10) and 1.33 (0.98-1.79), respectively. Defining $C_{peak}$ as the residuals of non-transformed *C* (NR model) resulted in more peaks detected when $C_{back}$ and variability was high ($s = 0.63$ [0.43-0.87]), and transforming and using an index to define $C_{peak}$ (TI model) resulted in nearly twice as many peaks detected when $C_{back}$ and variability were low ($s = 1.70$ [1.15-2.63]).

Overall, analyses of simulated records illustrate the sensitivity of decomposition methods to changes in the mean (Scenario 1) and changes in the mean and variance (Scenario 2) of a series through time. Although simplified, the sensitivity of the simulated

records to the analytical method highlights biases that can arise from similar changes in empirical records, even when of smaller magnitude and/or duration.

*Empirical Records*

The three empirical records differed greatly in their long-term variability in *C* (Fig 4). Little Lake had relatively low charcoal values until ca. 4000 yr BP when sediment accumulation rate increased five-fold (0.07 to 0.35 cm $yr^{-1}$) in parallel with *C*. At Rockslide Lake, sediment accumulation rates varied about two-fold (0.04 to 0.08 $yr^{-1}$) and were largely independent of *C*. At Ruppert Lake, sediment accumulation rates varied nearly five-fold (0.018 to 0.181 cm $yr^{-1}$) and while *C* followed the sediment accumulation rate during the first few millennia, these variables were unrelated for the majority of the record.

The raw records (*C*) at each site exhibited significant heteroscedasticity (Table 4), with Little Lake exhibiting the most, followed by Ruppert and Rockslide lakes ($W_{50}$ = 153.14, 84.62, 15.20, respectively; $p \leq 0.001$). The four detrending models had a large effect on the variance in $C_{peak}$ (Table 4; Fig. 4). The TR and NI models were most effective at stabilizing variance, although results differed between sites. At Rockslide Lake the TR model stabilized variance (500-2500 vs. 2500-0 yr BP, $W_{50}$ = 0.49, p = 0.483); this model performed second best at Little Lake (800-4000 vs. 4000-0 yr BP, $W_{50}$ = 3.40, p = 0.066) and performed worst at Ruppert Lake (10,000-5000 vs. 5000-0 yr BP, $W_{50}$ = 66.52, $p < 0.001$). At Little Lake, the NI model stabilized variance ($W_{50}$ = 0.01, p = 0.942), and at Ruppert Lake no model stabilized variance. Although the NR and TI models reduced heteroscedasticity, they did not stabilize variance in any record.

Skewness in $C_{peak}$ was largest when using the NR model (Little Lake, 17.73) or NI model (Rockslide and Ruppert lakes, 5.28, 6.79, respectively). In contrast, log-transforming $C$ (TR and TI models) reduced skewness, and at Little Lake these models resulted in near-symmetric distributions (0.28 and -0.56, respectively; Table 4).

The noise distribution fit by the Gaussian mixture model resulted in different signal-to-noise (SNI) and skewness values, dependent on the decomposition model (Fig. 5). As applied to the Rockslide Lake record, the NR and NI models yielded the largest signal-to-noise index (SNI; 0.97 and 0.98), whereas the TR and TI models had the smallest SNI (0.81 and 0.94). Skewness, as a potential measure of the occurrence of high values distinct from a noise distribution, was highest for the NI model (5.28). The TR model, though having a moderate SNI, was the most symmetric (skewness = 1.68).

As with simulated records, peak detection in empirical records was more sensitive to alternative decomposition models when using a global vs. local threshold, and this sensitivity varied greatly between sites (Fig. 6). At Little Lake, where $C_{back}$ varied the most throughout the record, a global threshold detected 41 peaks with the NR model but only 5 with the TI model, producing drastically different trends in 1000-yr mean fire frequency. The TR and NI models produced an intermediate number of peaks (23 and 30) with qualitatively similar trends over time. In contrast to Little Lake, peak detection with any model varied by 6% at Rockslide Lake (33-35) and 13% at Ruppert Lake (64-72), where variability in $C_{back}$ was less. At all sites, locally-defined thresholds detected more peaks and with less variability between models than with globally-defined thresholds, even after minimum-count screening (described below). Again, differences among models were greatest at Little Lake, where peak detection varied from 56-68 (21%). Peak

detection varied little at Rockslide Lake, 34-36 (6%), and slightly more at Ruppert Lake, 79-88 (11%). Differences at Little and Ruppert lakes largely reflect differences between the two residual models (NR and TR) in comparison to the index models (NI and TI).

The minimum-count screening flagged between 0-14% of the total peaks detected in any one record, with the least at Little Lake (median = 2.5%), followed by Rockslide Lake (median = 9%) and Ruppert Lake (median = 11%). A greater proportion of the total peaks detected was flagged when using a local vs. global threshold (median = 9% vs. 3%), and the variability between detrending models differed by threshold type. When using a global threshold, a larger percentage of total peaks were flagged when using index models (median for NI and TI = 11%) vs. residual models (median for NR and TR = 3%). This difference was reduced using a local threshold (10% vs. 9%, respectively).

## Discussion

Interpreting local fire history from sediment charcoal records involves a number of analytical steps that decompose multiple signals into a series of peaks that bears interpretation (Fig. 1). Accounting for non-stationarity in a record is a primary goal of decomposition methods, and our analyses of simulated records illustrate the sensitivity of alternative methods to two types of non-stationarity: a change in the mean (Scenario 1), and a change in the mean and variance (Scenario 2) through time. In combination with empirical records, our results highlight some critical methodological considerations that have been broadly overlooked in the literature. Specifically, we emphasize the need for careful consideration when proceeding through steps 4-6 of a decomposition method (Fig. 1): (a) defining $C_{peak}$, or detrending, (b) defining a threshold to detect peaks, and, in

the case of charcoal counts, (c) screening and removing peaks that could result from insignificant changes in charcoal counts.

*Detrending to define a peak series*

An overriding conclusion from our study is that the impacts of different detrending models are largely obviated by using a locally-defined threshold. In simulated records, peak identification using a local threshold was robust to changes in background charcoal, peak variance, and detrending model (Fig. 3). In empirical records, these patterns largely held true, as reflected by less between-model variability when using local vs. global thresholds. For example, the total number of peaks detected since 5000 yr BP in Ruppert Lake varied by 7% vs. 30% when applying a local vs. global threshold to the different detrending models (Fig. 6). Locally-defined thresholds outperformed global thresholds because the mixture model used to determine thresholds constantly adapts to variability in a record. Consequently, local thresholds are free from the assumption of stable variance in peak heights, at least for time scales longer than the window width used to define "local." With no need to stabilize variance across a record, detrending before applying a locally-defined threshold needs only to account for changes in the long-term mean, and thus three of the four detrending models evaluated become obsolete. Even stabilizing the mean, interestingly, may be unnecessary when using a locally-defined threshold, but no studies have attempted this to date. Our results are consistent with analyses done by Ali *et al.* (2009b), who applied the local threshold technique to three different charcoal quantification metrics from individual cores (counts, area, and estimated volume). Although the variability between the three metrics differed, the

locally-applied threshold produced similar results in each case. Overall, these findings lend support to the recent adoption of local thresholds for peak-identification (Table 1) as robust to changes in variance both within and between records.

Although local thresholds effectively eliminate the need to stabilize variance, understanding the impacts of detrending models when combined with global threshold remains important, mainly due to the prior use of these approaches (Table 1). Our results suggest that reanalysis of some previously-published records is justified, as has been initiated in some larger-scale synthesis studies (Marlon *et al.* 2009). In particular, analyses using a global threshold and the NR model with clearly heteroscedastic records or a global threshold with the TI model should be reconsidered, given the potential for systematically biased peak detection during periods of high or low $C_{back}$.

When applying a global threshold, it is imperative to evaluate the presence or absence of heteroscedasticity in a record before selecting a detrending model. If a record has stable variance, then the NR model is the single appropriate model because it only removes the mean trend of a series (Fig. 2). In simulated records, the only instance in which the global threshold was unbiased was when the NR model was applied to homoscedastic records (Scenario 1; Fig. 3). The closest analogy in the empirical records is from Rockslide Lake, which had the least heteroscedasticity of the three records evaluated (and was the shortest in length) and consequently was most robust to alternative detrending methods. Applying variance-stabilizing models (TR, NI, TI) to homoscedastic records is not only unwarranted, but it can result in severely biased peak identification (Fig. 3) by simultaneously amplifying and suppressing peaks during periods of low and high background charcoal, respectively (Fig. 2). This bias was

minimized when using the TR model, and it subsequently increased with the NI and TI models. By amplifying peak sizes when $C_{back}$ is low, index-based models applied to homoscedastic records result in biased peak identification (Fig. 2, 6). This bias is most extreme when using the TI model in combination with a global threshold, as this led to more than twice as many peaks being detected during periods of low vs. high background charcoal in our simulations (Fig. 3).

Unfortunately, most empirical charcoal records exhibit heteroscedasticity at some time scale, particularly those spanning different biomes and/or many millennia. This limits the utility of the NR model with a global threshold. All the empirical records in this study, for example, had non-stable variance between the two periods of comparison (Table 4; Fig. 4). In heteroscedastic records, both empirical and simulated records support the TR or NI models as most appropriate for consideration when using a global threshold. Although no model stabilized variance in the simulated records with heteroscedasticity, the TR and NI performed the best, and in empirical records these models stabilized variance across comparison periods in some records (Table 4). When applied to heteroscedastic records, the NR and TI models are inappropriate for the opposite reasons. Simply detrending by residuals (NR) fails to remove any heteroscedasticity (Table 4), which biases peak identification towards periods of high $C_{back}$ (Fig. 3). Detrending with an index of transformed data (TI) *reverses* the pattern of heteroscedasticity in what is essentially a "double whammy" of variance-stabilization (Fig. 2, 4), biasing peak identification towards periods of low $C_{back}$ (Fig 3). The undesirable effects of the TI model are most apparent in the Little Lake record, where four of the five peaks detect occurred during the period of low background charcoal (Fig.

6). The overall low number of peaks detect in this scenario also stands out as odd, and it highlights the conceptual difficulty of interpreting fire history from a symmetric peak series. If the variability above $C_{back}$ does not differ from the variability below $C_{back}$, then it is inconsistent to interpret the former as fire-related while interpreting the latter as noise-related. When a globally-defined Gussian mixture model is applied to a nearly symmetric peak series (e.g., Little Lake under the TI model, skewness = -0.56; Table 4), selecting a threshold at the 99$^{th}$ percentile cuts off 99% of the samples in the series (895 of 900 samples in the Little Lake record; Fig. 6).

Finally, we emphasize that the impacts of different detrending models will vary between sites, depending on the mean and variability of charcoal accumulation rates in a record. Rockslide Lake, for example, was largely robust to alternative decomposition methods, whereas Little Lake displayed large variability between methods (Fig. 7). Ruppert Lake was also clearly heteroscedastic, but overall lower $C$ and $C_{back}$ values as compared to Little Lake resulted in less sensitivity to alternative detrending models (Fig. 6).

*Defining a threshold*

The Gaussian mixture model introduced by Gavin *et al.* (2006) is promising because it provides a semi-objective, process-based means of selecting a threshold for peak identification which in turn can be applied to multiple records. Using the mixture model to identify a threshold depends upon three key assumptions: (1) variation in the noise distribution, representing variability around the long-term trend (i.e. $C_{back}$), is normally distributed; (2) the mean and variance of this noise distribution is stationary

within the period of analysis; and (3) there are enough samples within the period of analysis to adequately characterize the noise distribution. The first assumption has theoretical support from a charcoal simulation model (Fig. 3 in Higuera et. al. 2007), and it is consistent with the distributions of peak charcoal observed in empirical records (e.g. Higuera *et al.* 2009; Fig. 5). The mechanisms creating normally-distributed variability around the long-term trend include sediment mixing, inter-annual variability in long-distant charcoal input, sampling effects, and analytical error. Other mechanisms may produce skewed variability, and to the extent that this is true, this is a limitation of the Gaussian mixture model (discussed below).

The second assumption, that the properties of the noise distribution are stable, becomes increasingly difficult to satisfy as more samples are included in the population. The two ways to satisfy this assumption are to define the threshold over a period of stable mean and variance (i.e. use a locally-defined threshold), and/or define $C_{peak}$ with one of the two recommended variance-stabilizing methods (TR, NI). The shorter the period over which a threshold is defined, the more difficult it becomes to satisfy the third assumption, that the Gaussian distribution adequately describes the empirical data. Thus, the analyst has to make a trade-off between satisfying assumptions two and three. In practice, one can test the third assumption with a goodness-of-fit statistic, which quantifies the probability that the empirical data came from the modeled Gaussian distribution (e.g. Higuera *et al.* 2009). The modified Levene's test used in this study can be used to test for equal variance between different periods in a peak series. Future application of this test could be done on shorter, overlapping intervals, although one faces reduced statistical

power as the intervals decrease, and interpreting p-values become difficult with multiple comparisons.

The application of the Gaussian mixture model to identify a threshold is also aided by maximizing the separation between the noise distribution and fire-related peaks. This is a key difference between the analytical approach taken for peak identification compared to the analysis of long-term trends in total charcoal (e.g., Marlon *et al.* 2008, Power *et al.* 2008, Marlon *et al.* 2009). Whereas homogenizing variance is desirable in the context of the latter, this decreases separation between noise and fire-related samples, i.e., it reduced the signal-to-noise index (SNI). For example, in the Rockslide Lake record, the SNI was highest (0.97-0.988) using the NR and NI models, whereas it was consistently lowered when applying variance-stabilizing transformations (0.81-0.94; Fig. 5). Skewness may also serve as a coarse index of how separated peak values are from non-peak values. At Little Lake, a nearly symmetric peak distribution defined by the TI model reflected little to no separation between peak and non-peak values. Thus, as a general rule, a minimum level of skewness of around two would suggest a SNI sufficient to aid in setting thresholds, but increased skewness beyond two does not necessarily equate to an increased SNI. We also note that skewness alone is not justification for peak interpretation, particularly if it is an artifact of the detrending processes.

*Interpreting small charcoal peaks*

Most decomposition methods resulted in the identification of small peaks that failed to pass the minimum-count test at the 95% confidence level (0-14% of the total peaks identified; Fig. 6). Some peaks fail to past this test because they closely follow

other large peaks (i.e. a "double peak"), e.g., around 1200 yr BP at Ruppert Lake (Fig. 4 and 6). These peaks most likely represent non-significant variations in charcoal counts due to natural and/or analytical variability. More challenging for sediment-based fire-history reconstructions are periods of low charcoal abundance. In these cases, both variance-stabilizing and local-threshold methods may result in detecting small peaks, often associated with small charcoal counts in the raw record. The smaller the charcoal peak, the more difficult it is to infer if the peak was caused by a local fire vs. a distant fire and/or random variability in charcoal deposition and quantification. The minimum-count test helps guard against falsely inferring a peak was caused by a local fire (Type I error). When this probability is low, e.g. $< 0.05$, it is highly unlikely that the two samples come from the same population. Practically, Figure 7 illustrates the increase in counts (as a proportion and absolute number) required to achieve a given level of confidence (95 or 99%) as a function of the number of charcoal pieces in the pre-peak sample. The lower the pre-peak count, the greater the proportional increase in charcoal required before a peak sample can be considered distinct with 95% confidence. For example, when pre-peak counts are $< 10$, peak counts must double before having a $< 5\%$ chance of coming from the same populations. Much smaller proportional increases are required when overall counts are large, e.g., only a 20% increase is required when pre-peak sample are ca. 100. Thus, as a rough rule of thumb, it is highly desirable for researchers to use sample volumes that will result in average non-peak samples of $> 10$ pieces, and peak values of *at least* 20 pieces.

Even with large sample volume, in some cases the difference between a peak and non-peak sample may be small. Interpreting variability when charcoal counts are low

highlights a limitation of the Gaussian mixture model briefly mentioned above. The mixture model assumes normally-distributed noise, and thus it may fail when counts are small, because the true noise distribution may be positively skewed (i.e., Poisson distributions with a mean < 10 are positively skewed). If so, the Gaussian mixture model would underestimate the threshold, resulting in an increased false-positive rate. Future efforts modeling noise distributions within $C_{peak}$ could address this limitation through the use of non-Gaussian mixture models, which may be more appropriate for the heavy-tailed distributions that characterize $C$ and $C_{peak}$ series (Coles 2001). For example, the signal and noise distributions may be better fit by models in the generalized extreme value family (e.g., Weibull, Fréchet, and Gumbel distributions), and the signal distribution may be fit more appropriately by models in the Generalized Pareto family (e.g. Pareto, beta, and exponential distributions; Katz *et al.* 2005). In the ideal case, the signal distribution has little influence on the parameters of the noise distributions, because the noise population typically dominates the mixed distribution. Nonetheless, improving the fit of the signal distribution would be an improvement over current methods and deserves exploration. In the mean time, we suggest that the minimum-count test serves well to screen out small peaks, be they detected with a threshold from Gaussian mixture model or otherwise.

*Recommendations and Conclusions*

Even when applying the most rigorous analytical techniques, there is no substitute for careful inspection of a record to assess whether it can provide an unbiased fire history in the first place. We highlight three key issues related to assessing the quality of

millennial-scale charcoal records when independent evidence supporting a particular reconstruction is lacking. First, records should be interpreted in the context of a null hypothesis of random variability. If a peak series lacks large values, is symmetric, or fails to detect recent fires, then the record should be considered too noisy for peak identification. The signal-to-noise index utilized here is intended to help evaluate this null hypothesis, and current work is improving the application of this metric for this purpose (Kelly *et al.*, in preparation). Records with low SNI value(s) or symmetric peak series should either forgo peak identification methods, or be presented with a low, medium, and high ranges of possible thresholds. Depending on the cause of a low SNI, these records may still be appropriate and valuable for interpreting trends in biomass burning through interpretations of $C$ and/or $C_{back}$.

Second, if a record has large variability in sediment accumulation rates, practitioners must consider the possibility that changing peak frequencies result from changes in sample resolution. Resampling a record to the median or maximum deposition time per sample coarsens or falsely increases the resolution during periods of high or low sediment accumulation, and thus should create a more temporally unbiased time series. However, this resampling may not be a simple solution if sedimentation varies widely, because sediment mixing modifies the effect of changing sediment accumulation rate on the effective resolution of a sediment record. For example, mixing the top 2-cm of sediment during a period when the deposition time is 10 yr $cm^{-1}$ would result in an effective 1-cm resolution of 20 years. In contrast, the same 2-cm mixing depth during a sediment accumulation rate of 20 yr $cm^{-1}$ would result in an effective resolution of 40 years. An important cause of changing sediment accumulation rate is fluctuating within-

basin sediment focusing and sediment delivery by stream flow. Such processes can change the effectiveness of sediment delivery, including charcoal, from lake margins to the lake center. This results in the widely observed positive correlation between charcoal accumulation and sediment accumulation rates (i.e., constant charcoal concentration despite changing sediment accumulation rates) and a heteroscedastic charcoal record (e.g., Fig. 4). In contrast, if charcoal were delivered entirely through airfall, increased sediment accumulation rates would dilute charcoal concentrations, and the charcoal record would not be heteroscedastic. Therefore, we strongly warn against interpreting fire frequency changes in records with a several-fold change in sediment accumulation rate (along with no evidence that charcoal concentrations are diluted by changing sedimentation) and when inferred fire frequency closely tracks sediment accumulation rates. While there may be a non-causal relationship between sediment accumulation and fire frequency (e.g., via erosion or climate), this link must be explained with independent evidence if fire history is to be interpreted. A viable alternative in these cases is to only interpret high-resolution segments with constant sediment accumulation rates.

Finally, segments of records with low overall counts must be interpreted with caution. The use of the minimum-count test presented here can help guide interpretation in these cases, as can independent evidence of fire (e.g., pollen or macrofossils of fire-dependent taxa). While charcoal records have successfully detected fires in non-forested ecosystems (e.g. savannah and tundra: Duffin *et al.* 2008, Higuera *et al.* 2008b), at some point along a fire-intensity spectrum, fires will not produce enough charcoal to create an identifiable peak in a record (Higuera *et al.* 2005, Duffin *et al.* 2008). This may be the case even with ample sample volume. Likewise, as local fire frequency decreases, so too

does the frequency of large charcoal peaks; this makes it more difficult to identify the signal of local fires from the noise of long-distance transport and within-lake redeposition.

Following Clark's (1988a, 1988c) work in detecting fires from charcoal in laminated lake sediments, high-resolution charcoal records have proliferated in the absence of a thorough statistical framework for interpretation. This study is a first attempt to provide such a framework. We conclude from discussion above that applying a local threshold, in conjunction with the minimum-count test, is likely to provide the best interpretation of fire history from high-resolution macroscopic charcoal records. In most cases, the simplest detrending model (NR) is appropriate in this context, but there may be scenarios where the TR or NI variance-stabilization methods are justified. We emphasize the need for careful consideration when selecting, applying, and interpreting variance-stabilizing methods, and we encourage practitioners to evaluate the sensitivity of these choices on fire-history interpretations. Despite the challenges of inferring fire history from sediment charcoal records, significant progress has been made to improve the rigor of analysis and interpretations. In combination with the growing database of high-resolution charcoal records worldwide, charcoal records should continue to contribute uniquely to our understanding of fire regimes, the controls and ecological impacts of fire, and the role of fire in the Earth system.

**Acknowledgements**

We thank Doug Sprugel for raising these issues and Colin Long for sharing the Little Lake data.

## References


Ali, AA, H Asselin, AC Larouche, Y Bergeron, C Carcaillet, and PJH Richard (2008) Changes in fire regime explain the Holocene rise and fall of Abies balsamea in the coniferous forests of western Quebec, Canada. *Holocene* **18**, 693-703.

Ali, AA, C Carcaillet, and Y Bergeron (2009a) Long-term fire frequency variability in the eastern Canadian boreal forest: the influences of climate vs. local factors. *Global Change Biology* **15**, 1230-1241.

Ali, AA, PE Higuera, Y Bergeron, and C Carcaillet (2009b) Comparing fire-history interpretations based on area, number and estimated volume of macroscopic charcoal in lake sediments. *Quaternary Research* **72**, 462-468.

Allen, CD, RS Anderson, RB Jass, JL Toney, and CH Baisan (2008) Paired charcoal and tree-ring records of high-frequency Holocene fire from two New Mexico bog sites. *International Journal of Wildland Fire* **17**, 115-130.

Anderson, RS, CD Allen, JL Toney, RB Jass, and AN Bair (2008) Holocene vegetation and fire regimes in subalpine and mixed conifer forests, southern Rocky Mountains, USA. *International Journal of Wildland Fire* **17**, 96-114.

Anderson, RS, DJ Hallett, E Berg, RB Jass, JL Toney, CS de Fontaine, and A DeVolder (2006) Holocene development of Boreal forests and fire regimes on the Kenai Lowlands of Alaska. *Holocene* **16**, 791-803.

Beaty, RM, and AH Taylor (2009) A 14 000 year sedimentary charcoal record of fire from the northern Sierra Nevada, Lake Tahoe Basin, California, USA. *Holocene* **19**, 347-358.

Bretherton, CS, M Widmann, VP Dymnikov, JM Wallace, and I Blade (1999) The effective number of spatial degrees of freedom of a time-varying field. *Journal of Climate* **12**, 1990-2009.

Briles, CE, C Whitlock, and PJ Bartlein (2005) Postglacial vegetation, fire, and climate history of the Siskiyou Mountains, Oregon, USA. *Quaternary Research* **64**, 44-56.

Briles, CE, C Whitlock, PJ Bartlein, and PE Higuera (2008) Regional and local controls on postglacial vegetation and fire in the Siskiyou Mountains, northern California, USA. *Palaeogeography Palaeoclimatology Palaeoecology* **265**, 159-169.

Brown, MB, and AB Forsythe (1974) Robust Tests for Equality of Variances. *Journal of the American Statistical Association* **69**, 364-367.

Brunelle, A, and RS Anderson (2003) Sedimentary charcoal as an indicator of late-Holocene drought in the Sierra Nevada, California, and its relevance to the future. *The Holocene* **13**, 21-28.

Brunelle, A, and C Whitlock (2003) Postglacial fire, vegetation, and climate history in the Clearwater Range, northern Idaho, USA. *Quaternary Research* **60**, 307-318.

Brunelle, A, C Whitlock, P Bartlein, and K Kipfmueller (2005) Holocene fire and vegetation along environmental gradients in the Northern Rocky Mountains. *Quaternary Science Reviews* **24**, 2281-2300.

Carcaillet, C, Y Bergeron, PJH Richard, B Frechette, S Gauthier, and YT Prairie (2001) Change of fire frequency in the eastern Canadian boreal forests during the Holocene: does vegetation composition or climate trigger the fire regime? *Journal of Ecology* **89**, 930-946.

Clark, JS (1988a) Effects of climate change on fire regimes in northwestern Minnesota. *Nature* **334**, 233-235.

Clark, JS (1988b) Particle motion and the theory of charcoal analysis: source area, transport, deposition, and sampling. *Quaternary Research* **30**, 67-80.

Clark, JS (1988c) Stratigraphic charcoal analysis on petrographic thin sections: application to fire history in northwestern Minnesota. *Quaternary Research* **30**, 81-91.

Clark, JS (1990) Fire and climate change during the last 750 yr in northwestern Minnesota. *Ecological Monographs* **60**, 135-159.

Clark, JS, and WA Patterson. 1997. Background and local charcoal in sediments: scales of fire evidence in the paleorecord. Pages 23-48 *in* J. S. Clark, H. Cachier, J. G. Goldammer, and B. J. Stocks, editors. Sediment Records of Biomass Burning and Global Change. Springer, New York.

Clark, JS, and PD Royall (1996) Local and regional sediment charcoal evidence for fire regimes in presettlement north-eastern North America. *Journal of Ecology* **84**, 365-382.

Clark, JS, PD Royall, and C Chumbley (1996) The role of fire during climate change in an eastern deciduous forest at Devil's Bathtub, New York. *Ecology* **77**, 2148-2166.

Cleveland, WS (1979) Robust locally weighted regression and smoothing scatterplots. *Journal of the American Statistical Association* **74**, 829-836.

Coles, S (2001) An introduction to statistical modeling of extreme values. Springer-Verlag, London, UK.

Cook, ER, and K Peters (1997) Calculating unbiased tree-ring indices for the study of climatic and environmental change. *The Holocene* **7**, 359-368.

Daniels, ML, RS Anderson, and C Whitlock (2005) Vegetation and fire history since the Late Pleistocene from the Trinity Mountains, northwestern California, USA. *Holocene* **15**, 1062-1071.

Davis, MB, RE Moeller, and J Ford. 1984. Sediment focusing and pollen influx. Pages 261-293 *in* E. Y. Haworth and J. W. G. Lund, editors. Lake Sediments and Environmental History. University of Leicester Press, Leicester, U.K.

Detre, K, and C White (1970) Comparison of 2 Poisson-Distributed Observations. *Biometrics* **26**, 851-&.

Duffin, KI, L Gillson, and KJ Willis (2008) Testing the sensitivity of charcoal as an indicator of fire events in savanna environments: quantitative predictions of fire proximity, area and intensity. *Holocene* **18**, 279-291.

Emerson, JD. 1983. Mathematical aspects of transformation

Pages 247-282 *in* D. C. Hoaglin, F. Mosteller, and J. W. Tukey, editors. Understanding Robust and Exploratory Data Analysis. Wiley

Fowler, AM (2009) Variance Stabilization Revisited: A Case for Analysis Based on Data Pooling. *Tree-Ring Research* **65**, 129-145.

Gavin, DG, LB Brubaker, and KP Lertzman (2003) An 1800-year record of the spatial and temporal distribution of fire from the west coast of Vancouver Island, Canada. *Canadian Journal of Forest Research* **33**, 573-586.

Gavin, DG, DJ Hallett, FS Hu, KP Lertzman, SJ Prichard, KJ Brown, JA Lynch, P Bartlein, and DL Peterson (2007) Forest fire and climate change in western North

America: insights from sediment charcoal records. *Frontiers in Ecology and the Environment* **5**, 499-506.

Gavin, DG, FS Hu, K Lertzman, and P Corbett (2006) Weak climatic control of stand-scale fire history during the late Holocene. *Ecology* **87**, 1722-1732.

Giesecke, T, and SL Fontana (2009) Revisiting pollen accumulation rates from Swedish lake sediments. *The Holocene* **18**, 293-305.

Hallett, DJ, and RS Anderson (2010) Paleo-fire reconstruction for high-elevation forests in the Sierra Nevada, California with implications for wildfire synchrony and climate variability in the late Holocene. *Quaternary Research* **73**, 180-190.

Hallett, DJ, DS Lepofsky, RW Mathewes, and KP Lertzman (2003a) 11,000 years of fire history and climate in the mountain hemlock rain forests of southwestern British Columbia based on sedimentary charcoal. *Canadian Journal of Forest Research* **33**, 292-312.

Hallett, DJ, RW Mathewes, and RC Walker (2003b) A 1000-year record of forest fire, drought and lake-level change in southeastern British Columbia, Canada. *Holocene* **13**, 751-761.

Hallett, DJ, and RC Walker (2000) Paleoecology and its application to fire and vegetation management in Kootenay National Park, British Columbia. *Journal of Paleolimnology* **24**, 401-414.

Higuera, PE, LB Brubaker, PM Anderson, TA Brown, AT Kennedy, and FS Hu (2008a) Frequent Fires in Ancient Shrub Tundra: Implications of Paleorecords for Arctic Environmental Change. *PLoS ONE* **3**, e0001744.

Higuera, PE, LB Brubaker, PM Anderson, FS Hu, and TA Brown (2009) Vegetation mediated the impacts of postglacial climate change on fire regimes in the south-central Brooks Range, Alaska. *Ecological Monographs* **79**, 201-219.

Higuera, PE, M Chipman, JA Allen, S Rupp, and FS Hu (2008b) Tundra fire regimes in the Noatak National Preserve, northwestern Alaska, since 6000 yr BP. Pages 144 *in* 93th Annual Meeting of the Ecological Society of America, Milwaukee, WI.

Higuera, PE, ME Peters, LB Brubaker, and DG Gavin (2007) Understanding the origin and analysis of sediment-charcoal records with a simulation model. *Quaternary Science Reviews* **26**, 1790-1809.

Higuera, PE, DG Sprugel, and LB Brubaker (2005) Reconstructing fire regimes with charcoal from small-hollow sediments: a calibration with tree-ring records of fire. *The Holocene* **15**, 238-251.

Huber, UM, V Markgraf, and F Schäbitz (2004) Geographical and temporal trends in Late Quaternary fire histories of Fuego-Patagonia, South America. *Quaternary Science Reviews* **23**, 1079-1097.

Huerta, MA, C Whitlock, and J Yale (2009) Holocene vegetation-fire-climate linkages in northern Yellowstone National Park, USA. *Palaeogeography, Palaeoclimatology, Palaeoecology* **271**, 170-181.

Katz, RW, GS Brush, and MB Parlange (2005) Statistics of extremes: modeling ecological disturbances. *Ecology* **86**, 1124-1134.

Long, CJ, and C Whitlock (2002) Fire and vegetation history from the coastal rain forest of the western Oregon Coast Range. *Quaternary Research* **58**, 215-225.

Long, CJ, C Whitlock, and PJ Bartlein (2007) Holocene vegetation and fire history of the Coast Range, western Oregon, USA. *Holocene* **17**, 917-926.

Long, CJ, C Whitlock, PJ Bartlein, and SH Millspaugh (1998) A 9000-year fire history from the Oregon Coast Range, based on a high-resolution charcoal study. *Canadian Journal of Forest Research* **28**, 774-787.

Lynch, JA, JS Clark, NH Bigelow, ME Edwards, and BP Finney (2002) Geographic and temporal variations in fire history in boreal ecosystems of Alaska. *Journal of Geophysical Research* **108**, FFR8-1-FFR8-17.

Lynch, JA, JS Clark, and BJ Stocks (2004a) Charcoal production, dispersal and deposition from the Fort Providence experimental fire: Interpreting fire regimes from charcoal records in boreal forests. *Canadian Journal of Forest Research* **34**, 1642-1656.

Lynch, JA, JL Hollis, and FS Hu (2004b) Climatic and landscape controls of the boreal forest fire regime: Holocene records from Alaska. *Journal of Ecology* **92**, 447-489.

Marlon, J, PJ Bartlein, and C Whitlock (2006) Fire-fuel-climate linkages in the northwestern USA during the Holocene. *The Holocene* **16**, 1059-1071.

Marlon, JR, PJ Bartlein, C Carcaillet, DG Gavin, SP Harrison, PE Higuera, F Joos, MJ Power, and IC Prentice (2008) Climate and human influences on global biomass burning over the past two millennia. *Nature Geoscience* **1**, 697-702.

Marlon, JR, PJ Bartlein, MK Walsh, SP Harrison, KJ Brown, ME Edwards, PE Higuera, MJ Power, C Whitlock, RS Anderson, C Briles, A Brunelle, C Carcaillet, M Daniels, FS Hu, M Lavoie, C Long, T Minckley, PJH Richard, SL Shafer, W Tinner, and C Umbanhowar (2009) Wildfire responses to abrupt climate change in North America.

*Proceedings of the National Academy of Sciences of the United States of America* **106**, 2519-2524.

Millspaugh, SH, and C Whitlock (1995) A 750-year fire history based on lake sediment records in central Yellowstone National Park, USA. *The Holocene* **5**, 283-292.

Millspaugh, SH, C Whitlock, and P Bartlein (2000) Variations in fire frequency and climate over the past 17000 yr in central Yellowstone National Park. *Geology* **28**, 211-214.

Minckley, TA, C Whitlock, and PJ Bartlein (2007) Vegetation, fire, and climate history of the northwestern Great Basin during the last 14,000 years. *Quaternary Science Reviews* **26**, 2167-2184.

Mohr, JA, C Whitlock, and CN Skinner (2000) Postglacial vegetation and fire history, eastern Klamath Mountains, California, USA. *The Holocene* **10**, 587-602.

Mudelsee, M (2006) CLIM-X-DETECT: A Fortran 90 program for robust detection of extremes against a time-dependent background in climate records. *Computers & Geosciences* **32**, 141-144.

Power, MJ, J Marlon, N Ortiz, et al. (2008) Changes in fire regimes since the Last Glacial Maximum: an assessment based on a global synthesis and analysis of charcoal data. *Climate Dynamics* **30**, 887-907.

Power, MJ, C Whitlock, P Bartlein, and LR Stevens (2006) Fire and vegetation history during the last 3800 years in northwestern Montana. *Geomorphology* **75**, 420-436.

Prichard, SJ, Z Gedalof, WW Oswald, and DL Peterson (2009) Holocene fire and vegetation dynamics in a montane forest, North Cascade Range, Washington, USA. *Quaternary Research* **72**, 57-67.

Shiue, W, K., and LJ Bain (1982) Experiment size and power comparisons for two-sample Poisson tests. *Journal of Applied Statistics* **31**, 130-134.

Toney, JL, and RS Anderson (2006) A postglacial palaeoecological record from the San Juan Mountains of Colorado USA: fire, climate and vegetation history. *Holocene* **16**, 505-517.

Tweiten, MA, SC Hotchkiss, RK Booth, RR Calcote, and EA Lynch (2009) The response of a jack pine forest to late-Holocene climate variability in northwestern Wisconsin. *Holocene* **19**, 1049-1061.

Underwood, AJ ( 1997) Experiments in Ecology. Cambridge University Press, Cambridge.

Walsh, MK, C Whitlock, and PJ Bartlein (2008) A 14,300-year-long record of fire-vegetation-climate linkages at Battle Ground Lake, southwestern Washington. *Quaternary Research* **70**, 251-264.

Whitlock, C, W Dean, J Rosenbaum, L Stevens, S Fritz, B Bracht, and M Power (2008) A 2650-year-long record of environmental change from northern Yellowstone National Park based on a comparison of multiple proxy data. *Quaternary International* **188**, 126-138.

Whitlock, C, and C Larsen. 2001. Charcoal as a fire proxy. *in* J. P. Smol, H. J. B. Birks, and W. M. Last, editors. Tracking Environmental Change Using Lake Sediments. Kluwer Academic Publisher, Dordrecht.

## Tables

**Table 1**. Published fire-history studies in North America based on macroscopic charcoal (sieved or in thin sections) where the goal of analysis was to detect peaks associated with local fires. Studies are grouped by threshold type and the detrending models used for analysis. "N" indicates the total number of studies in each category.

| Threshold type | Detrending model | Citation | Location (State or Province) | Particle Count or Area | Sediment volume per sample ($cm^3$) | Size class tallied | Background estimate | Threshold determination[1] | Threshold value [2] |
|---|---|---|---|---|---|---|---|---|---|
| **Global** N = 37 | **Non-transform, Residuals (NR)** N = 13 | Clark (1990) | Minnesota, USA | A | Thin sections | > 60 µm long | 15-yr moving average | Three lakes: TR (2-8) | > 42 to 68 |
| | | Millspaugh and Whitlock (1995) | Wyoming, USA | C | 5 | 125 µm | 3-point, center weighted average | Five lakes: TR (2-8) | ≥ 3.4, > 4.6, ≥ 5 |
| | | Clark *et al.* (1996) | New York, USA | A | Thin sections | > 60 µm long | Inverse Fourier transform: 30-yr window | TR (11) | > 60 |
| | | Clark and Royall (1996) | New York, Wisconsin, Pennsylvania, Maine, USA Ontario, Canada | A | Thin sections | > 60 µm long | Inverse Fourier transform: 10-yr window | Seven lakes: H, TR | > 40 |
| | | Carcaillet *et al.* (2001) | Québec, Canada | A | 1 | >150 µm | Inverse Fourier transform: 100 yr window | Three lakes: TR: not possible | > 1sd of the average of background |
| | | Gavin *et al.* (2003) | British Columbia, Canada | C | ca. 12 | 150-500 µm | 26-yr locally weighted minimum value | SC (12), TR (3); S1 | 0.22 |
| | | Lynch *et al.* (2002) | Alaska, USA | A | 1 | >180 µm | 100-yr locally weighted mean | Three lakes: H (2); S1 | 0.07: upper 12% tail of residuals |
| | | Lynch *et al.* (2004a) | Alaska, USA; Manitoba, Northwest Territories, Ontario, Canada | A | 1 | >180 µm | 100-yr locally weighted mean | Fiftee lakes: H(1-2) for each lake; S1 | 0.03-0.33; upper 8-13% of residuals |

| | | | | | | | | |
|---|---|---|---|---|---|---|---|---|
| | Lynch *et al.* (2004b) | Alaska, USA | A | 1 to 3 | >180 µm | 100-yr locally weighted mean | Four lakes: S1 | 0.018, 0.085 |
| | Gavin *et al.* (2006) | British Columbia, Canada | C | 2 to 5 | >125 µm | 500-yr robust Lowess | Two lakes: H, TR (2); S1 | GMM; 0.08, 5.00 |
| | Prichard *et al.* (2009) | Washington, USA | C | ca. 10 | >150-500 µm | 750-yr locally weighted mean | TR (2): S1 | GMM at 99$^{th}$ percentile: not reported |
| | Ali *et al.* (2008) | Québec, Canada | A | 1 | > 160 µm | 500-yr tricube locally-weighted regression | Lake, peat and soil charcoal compared; S1 | GMM at 95$^{th}$ percentile: 0.2 |
| | Ali *et al.* (2009a) | Québec, Canada | A | 1 | > 160 µm | 1000-yr tricube locally-weighted regression | Four lakes: S1 | GSM at 95$^{th}$ percentile: 0.015, 0.025, 0.040, 0.007 |
| **Transform, Residuals (TR)** N = 1 | Hallett and Anderson (2010) | California, USA | C | 2.5 | > 125 µm | 500-yr robust Lowess | Two lakes: TR (1-2): S1 | GSM at 95$^{th}$ percentile: 0.03 |
| **Non-transform, Index (NI)** | Higuera *et al.* (2005) | Washington, USA | C | 3 | 150-500, > 500 µm | Series median (300-yr) | 12 Small hollows: TR (1-3 per site) | 1.63-1.75 |
| N = 2 | Tweiten *et al.* (2009) | Wisconsin, USA | C | 1 | > 150 µm | 300-yr Lowess | not possible | 1.3 |
| **Transform, Index (TI)** N = 22 | Long *et al.* (1998) | Oregon, USA | C | 2.5 | >125 µm | 600-yr locally-weighted mean | TR, H (4) | 1.12 |
| | Hallett and Walker (2000) | British Columbia, Canada | C, A | 1 | >150 µm | 500-yr locally weighted mean | TR (2) | 1.0 |
| | Millspaugh *et al.* | Wyoming, USA | C | 5 | >125 µm | 750-yr locally- | S2 | 1.0 |

| | | | | | | | |
|---|---|---|---|---|---|---|---|
| (2000) | | | | | weighted mean | | |
| Mohr *et al.* (2000) | California, USA | C | 5 | >125 µm | 120-yr locally-weighted mean | Two lakes: TR (3) | 1.0 |
| Long and Whitlock (2002) | Oregon, USA | C | 2.5 | >125 µm | 600-yr locally-weighted mean | H (2) | 1.25 |
| Brunelle and Anderson (2003) | California, USA | C | 5 | >125 µm | 500-yr locally-weighted mean | H(1) | 1.1 |
| Brunelle *et al.* (2003, 2005) | Idaho and Montana, USA | C | 5 | >125 µm | 750 or 600-yr locally-weighted mean | Four lakes: TR (3-5) | 1.15-1.30 |
| Hallett *et al.* (2003a) | British Columbia, Canada | C | 10 | >125 µm | 400-yr locally-weighted mean | Two lakes: SC (10-18) | 1.0 |
| Hallett *et al.* (2003b) | British Columbia, Canada | C | 10 | >125 µm | 50-yr locally-weighted mean | TR (4) | 1.1 |
| Daniels *et al.* (2005) | California, USA | C | ca. 8 | >125 µm | 370-yr locally-weighted mean | TR (3) | 1.0 |
| Briles *et al.* (2005) | Oregon, USA | C | 2 to 5 | >125 µm | 500-yr locally-weighted mean | TR (3) | 1.1 |
| Toney and Anderson (2006) | Colorado, USA | C | 5 | >125 µm | 300-yr locally-weighted mean | H (1) | 1.0 |
| Anderson *et al.* (2006) | Alaska, USA | C | 5 | >125 µm | 300-yr locally-weighted mean | H (3-5); SC (4) | 1.2 |
| Power *et al.* (2006) | Montana, USA | C | 0.3 to 1? | >125 µm | 150-yr locally- | H (1) | 1.05 |

| | | | | | | | | | |
|---|---|---|---|---|---|---|---|---|---|
| | | | | | | | weighted mean | | |
| | | Marlon *et al.* (2006) | California, Oregon, Montana, Wyoming, Idaho, USA | C | 1 to 5 | >125 µm | 500-yr locally-weighted mean | 15 lakes: H (1-5); TR (1-5); varies by site | 1.0-1.3 |
| | | Long *et al.* (2007) | Oregon, USA | C | 3 to 5 | >125 µm | 600-yr locally weighted mean | H (2-3); S1 | 1.2 |
| | | Anderson *et al.* (2008) | Colorado, New Mexico, USA | C | 1 to 5 | >125 µm | 1000-yr locally-weighted mean | Three lakes and three bogs: H (1-3) | 1.01 |
| | | Allen *et al.* (2008) | New Mexico, USA | C | 1 to 5 | >125 µm | 300-yr locally-weighted mean | Two bogs: TR (1-4), H (fire-free interval) | 1.01 |
| | | Minckley *et al.* (2007) | Oregon and California, USA | C | 4 to 5 | >125 µm | 900-yr locally-weighted mean | Three lakes: H (lowest threshold with no fires in last 100 yr) | 1.00, 1.05, 1.15 |
| | | Whitlock *et al.* (2008) | Wyoming, USA | C | 1 | >125 µm | 150-yr locally-weighted mean | TR (2) | 1.1 |
| | | Beaty and Taylor (2009) | California, USA | C | 3 | >125 µm | 240-yr locally-weighted mean | TR (3) | 1.0 |
| **Local** N = 6 | **Non-transform, Residuals (NR)** N = 6 | Higuera *et al.* (2008a) | Alaska, USA | C | 3 to 5 | >150 µm | smoothed 500-yr median or mode | Two lakes (pre-modern): S2 | GMM at 99$^{th}$ percentile |
| | | Walsh *et al.* (2008) | Washington, USA | C | 1 | >125 µm | 500-yr robust Lowess | TR (3); S2 | GMM at 95$^{th}$ percentile |
| | | Briles *et al.* (2008) | California, USA | C | 2 | >125µm | 700-yr locally-weighted regression | Two lakes; S2 | GMM at 95$^{th}$ percentile |
| | | Marlon *et al.* (2009) | North America | C | Varies with several records used | >125 µm | 500, 600, 800-yr robust Lowess | Thirty-five lakes: S2 | GMM at 95$^{th}$ percentile |
| | | Higuera *et al.* (2009) | Alaska, USA | C | 3 to 5 | >150 µm | smoothed | Four lakes: H(1); S2 | |

| | | | | | | | | |
|---|---|---|---|---|---|---|---|---|
| | | | | | | 500-yr median or mode | | GMM at 99th percentile |
| | Huerta *et al.* (2009) | Wyoming, USA | C | 5 and 50 | >125 μm | 500-yr robust Lowess | H(1); S2 | GMM at 95th percentile |

[1] Methods of threshold determination as follows:
TR: detected peaks compared to fires reconstructed from tree-rings (fire scars and/or stand ages)
SC: detect peaks compared to radiocarbon dates from local soil charcoal
H: detected peaks compared to historical fire record
S1: sensitivity analysis based on coefficient quantifying separation of peaks from background
S2: sensitivity analysis based on qualitative assessment of results using alternative threshold criteria
For TR, SC, and H methods, the number of independent fire records is shown in parentheses.

[2] Threshold values: Units for NR and TR models are pieces $cm^{-2}\ yr^{-1}$ for counts or $mm^2\ cm^{-2}\ yr^{-1}$ for area.
Thresholds for NI and TI models are unitless index values.
GMM: Gaussian mixture model. For local thresholds, the percentile of the GMM defines a different threshold value for each sample, and thus threshold values are not reported.
GSM: Gaussian single model, with mean of zero.

**Table 2**. Decisions typically required to develop a high-resolution lake-sediment macroscopic charcoal record, summarized from Whitlock and Larsen (2001). The aim of the current paper is to discuss data manipulations after completing these steps of developing a charcoal record.

| Step | Decisions | Potential issues and sources of error |
|---|---|---|
| 1. Sediment collection | Coring location | Gaps in record |
| 2. Sediment subsampling | Sediment volume per sample | Volume overestimate (core shrinkage). |
| | Sampling interval | Sample volume too small, resulting in low charcoal counts. |
| | | Interval too long to distinguish consecutive fire events. |
| 3. Sediment sieving | Sieve sizes | Incomplete sieving |
| | | Sample spillage |
| 4. Charcoal quantification | Count or area | Misidentification |
| | | Breakage of charcoal results in inflated counts. |
| 5. Estimate charcoal accumulation rate (CHAR) | Age-depth model fitting to calculate sediment accumulation rates | Poor chronological control |
| 6. Interpolate CHAR to a constant interval | Interval size (typical value is the median sample deposition time) | Loss of resolution in portions of the record |

**Table 3.** Selected abbreviations used in the text and corresponding definitions.

| Abbreviation | Definition |
|---|---|
| **Components of a Charcoal Record** | |
| $C$ | Resampled charcoal in a charcoal series, expressed as pieces $cm^{-2}$ $yr^{-1}$ or $cm^2$ $cm^{-2}$ $yr^{-1}$ |
| $\log(C+1)$ | Natural logarithm of resampled charcoal, after one is added to guard against negative values |
| $C_{back}$ | Background charcoal, defined as a function of resampled charcoal |
| $C_{back}$, where $C_{back}$ = f(log[C+1]) | Background charcoal, defined as a function of log-transformed, resmpled charcoal |
| $C_{peak}$ | Detrended, or "peak" series of a charcoal record, after trends in background charcoal are removed |
| **Detrending Models** | |
| NR | No-transform, Residual: $C_{peak} = C - C_{back}$ |
| NI | No-transform, Index: $C_{peak} = C / C_{back}$ |
| TR | Transform, Residual: $C_{peak} = \log(C+1) - C_{back}$, where $C_{back}$ = f(log[C+1]) |
| TI | Transform, Index: $C_{peak} = \log(C+1) / C_{back}$, where $C_{back}$ = f(log[C+1]) |

**Table 4.** Stationarity of variance and skewness of $C$ and $C_{peak}$ series for different decomposition models. The modified Levene's test statistic, $W_{50}$, and the probability of the null hypothesis of equal variances, p, are based on comparisons between values from 10,000-6000 to 4000-0 yr BP in simulated records, and equally split halves since 8000, 5000, and 10,000 yr BP for Little, Rockslide, and Ruppert lakes, respectively. Bold (italic) values identify stationary series, those that fail to reject the null hypothesis at α = 0.10 (0.05), where a higher α is more conservative. The skewness coefficient is a measure of the asymmetry of the entire peak series of each respective model, where positive values indicate greater spread above the mean value and a zero value indicates a symmetric distribution. The time series for each model is shown in Fig. 2 and 4 for the simulated and empirical records, respectively. Values for simulated records represent the median value from 500 records constructed under each scenario.

| **Scenario or Site** | **$W_{50}$ test statistic for equality of variances (p-value)** | | | | | **Skewness coefficient ($2.5^{th}$-$97.5^{th}$ percentile) [within-row rank]** | | | |
|---|---|---|---|---|---|---|---|---|---|
| | *C* | NR | TR | NI | TI | NR | TR | NI | TI |
| Scenario 1 (variance constant) | ***0.45 (0.502)*** | ***0.44 (0.508)*** | 46.72 (<0.001) | 25.62 (<0.001) | 98.54 (<0.001) | 2.59 (1.98-4.17) [1] | 0.96 (0.68-1.29) [2] | 3.47 (2.40-6.14) [1] | 1.22 (0.79-1.74) [2] |
| Scenario 2 (variance proportional) | 21.87 (<0.001) | 20.90 (<0.001) | 7.12 (0.008) | 10.81 (0.001) | 57.92 (<0.001) | 2.97 (2.12-5.05) [1] | 1.20 (0.89-1.52) [2] | 3.03 (2.17-4.98) [1] | 1.55 (1.01-2.10) [2] |
| Little Lake | 153.14 (<0.001) | 37.72 (<0.001) | *3.40 (0.066)* | ***0.01 (0.942)*** | 68.79 (<0.001) | 17.73 [1] | 0.28 [3] | 4.17 [2] | -0.56 [4] |
| Rockslide Lake | 15.20 (<0.001) | 5.71 (0.018) | ***0.49 (0.483)*** | 6.20 (0.013) | 14.70 (<0.001) | 3.16 [3] | 1.68 [4] | 5.28 [1] | 3.70 [2] |
| Ruppert Lake | 84.62 (<0.001) | 59.51 (<0.001) | 66.52 (<0.001) | 5.62 (0.018) | 9.11 (0.003) | 4.10 [3] | 3.14 [4] | 6.79 [1] | 6.37 [2] |

**Figure Legends**

**Fig. 1.** The set of decisions required for analyzing a charcoal time series with the goal of peak detection for interpretation of fire episodes. These steps are implemented in the *CharAnalysis* software (http://Charanalysis.googlepages.com; last accessed Oct 20, 2009).

**Fig. 2.** Simulated charcoal records reflecting alternative assumptions regarding the stability of the variance through time. (a) Representative records from each scenario. Scenario 1 has constant variance peak heights superimposed on a changing mean. Scenario 2 is a heteroscedastic series in which the peak variance changes in proportion to $C_{back}$. The thick black line in all figures is a 500-year loess smooth used to define the "background" levels ($C_{back}$). (b) Series expressed on a log scale. (c-f) Detrended series based on four alternative methods.

**Fig. 3.** Sensitivity of peak identification to decomposition models and threshold type. The sensitivity index, *s*, is the ratio of detected peaks from period 1 to period 2 in the two simulated charcoal scenarios in Fig 2. The error bars indicate the 95% confidence interval from 500 realizations of the simulated records.

**Fig 4.** Empirical charcoal records detrended using the four decomposition models. Records are from western Oregon (Little Lake; Long *et al.* 1998), southeast British Columbia (Rockslide Lake, Gavin *et al.* 2006), and the Alaskan Brooks Range (Ruppert Lake; Higuera *et al.* 2009).

**Fig 5.** The Gaussian mixture model applied to the $C_{peak}$ series from Rockslide Lake. Each panel corresponds to a single detrending model. The Gaussian model representing the noise

distribution is shown by a thick gray line. The vertical line represents a typical threshold level for peak identification, located at the 99$^{th}$ percentile of the lower distribution.

**Fig 6.** Inferred fire history from Little, Rockslide, and Ruppert lakes using alternative decomposition methods. Each row corresponds to a different detrending model, as in Fig. 4, and each panel includes peaks detected based on a global and local threshold. The location of peaks exceeding the threshold value(s) are identified with "+" and "." symbols, where the latter identifies peaks that failed to pass the minimum-count test. The proportion of total peaks failing to pass the minimum-count test is displayed on the right hand side of each panel. Smoothed lines represent the 1000-yr average fire frequency for a given decomposition method, and all panels are scaled from 0 to 15 (fires per 1000 yr) on the y-axis.

**Fig 7.** Minimum increase in charcoal counts required to confidently separate pre-peak from peak samples. The required increase is displayed as a total number and a proportion, and it depends upon (a) the confidence desired ($\alpha = 0.01$, 99% or $\alpha = 0.05$, 95% confidence), and (b) the number of pieces in the smaller, pre-peak sample. The curves are developed from the test for assessing whether two samples are from the same Poisson distribution (Detre and White 1970). Lines for two significance levels are shown and presented both as absolute counts and percentage increase of the lower count.

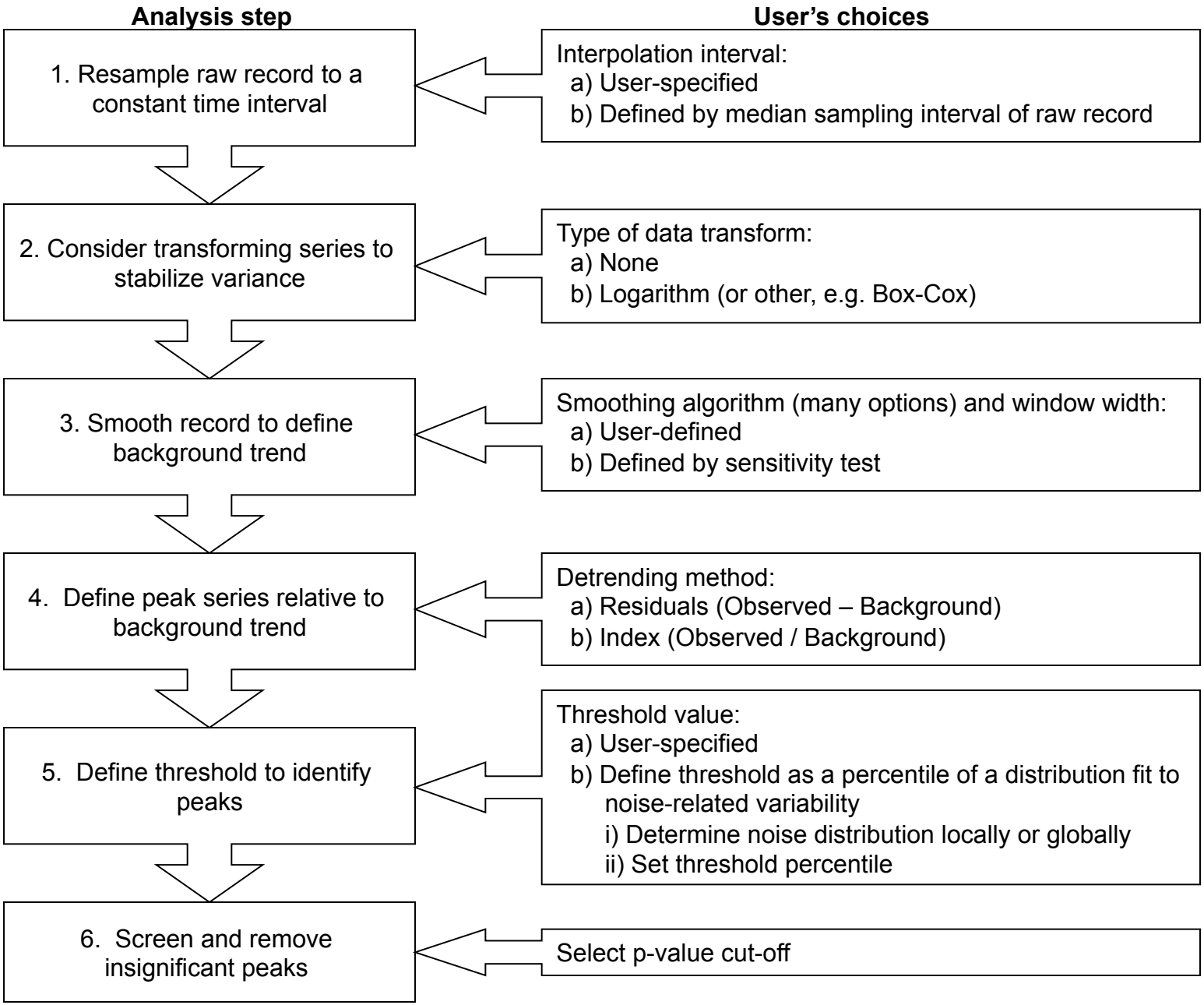
Analysis step
User's choices
1. Resample raw record to a constant time interval
Interpolation interval:
a) User-specified
b) Defined by median sampling interval of raw record
2. Consider transforming series to stabilize variance
Type of data transform:
a) None
b) Logarithm (or other, e.g. Box-Cox)
3. Smooth record to define background trend
Smoothing algorithm (many options) and window width:
a) User-defined
b) Defined by sensitivity test
4. Define peak series relative to background trend
Detrending method:
a) Residuals (Observed – Background)
b) Index (Observed / Background)
5. Define threshold to identify peaks
Threshold value:
a) User-specified
b) Define threshold as a percentile of a distribution fit to noise-related variability
i) Determine noise distribution locally or globally
ii) Set threshold percentile
6. Screen and remove insignificant peaks
Select p-value cut-off

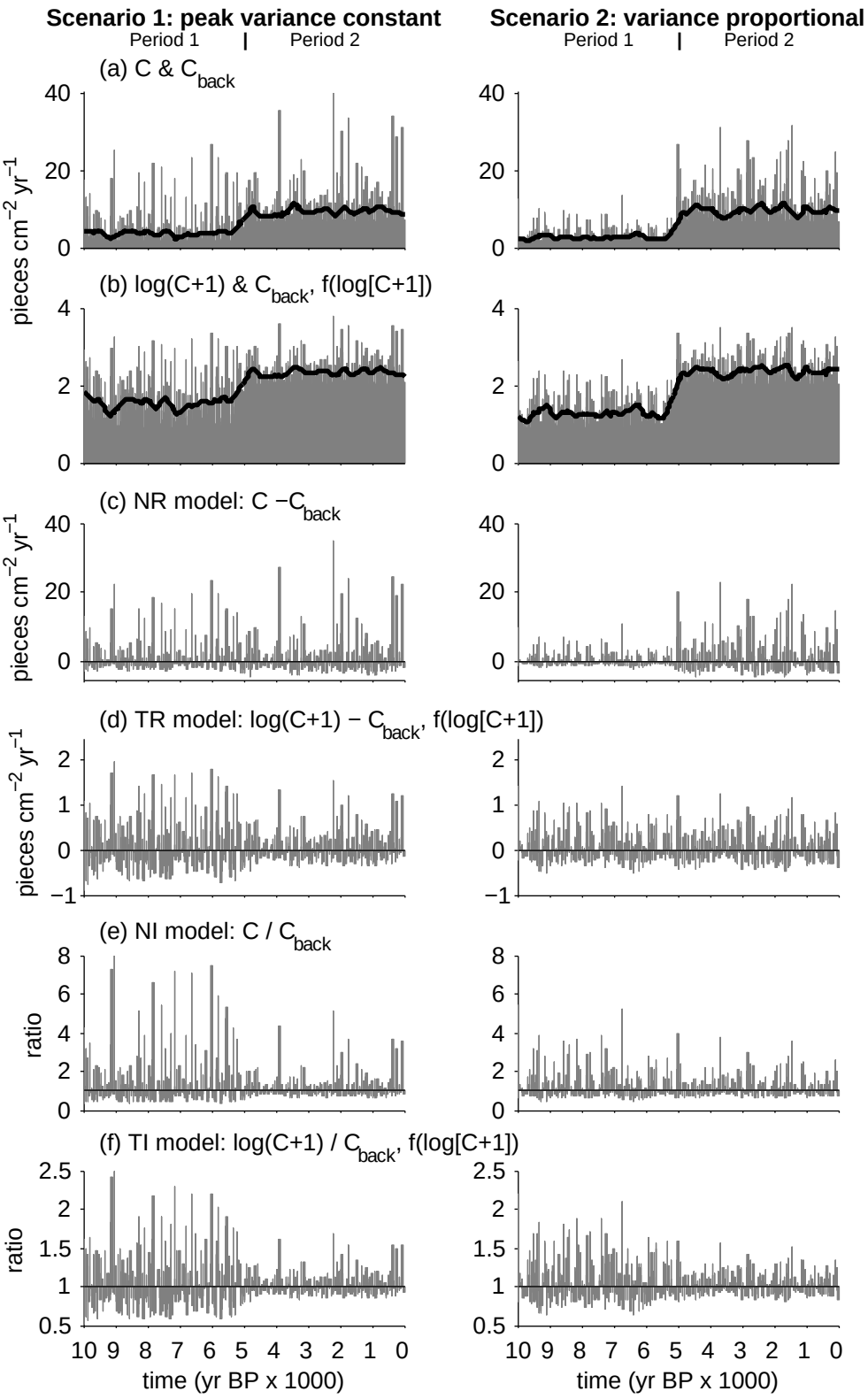
Scenario 1: peak variance constant
Period 1
Period 2
Scenario 2: variance proportional
Period 1
Period 2
(a) C & C back
(b) log(C+1) & C back, f(log[C+1])
(c) NR model: C −C back
(d) TR model: log(C+1) − C back, f(log[C+1])
(e) NI model: C / C back
(f) TI model: log(C+1) / C back, f(log[C+1])
pieces cm−2 yr−1
ratio
time (yr BP x 1000)

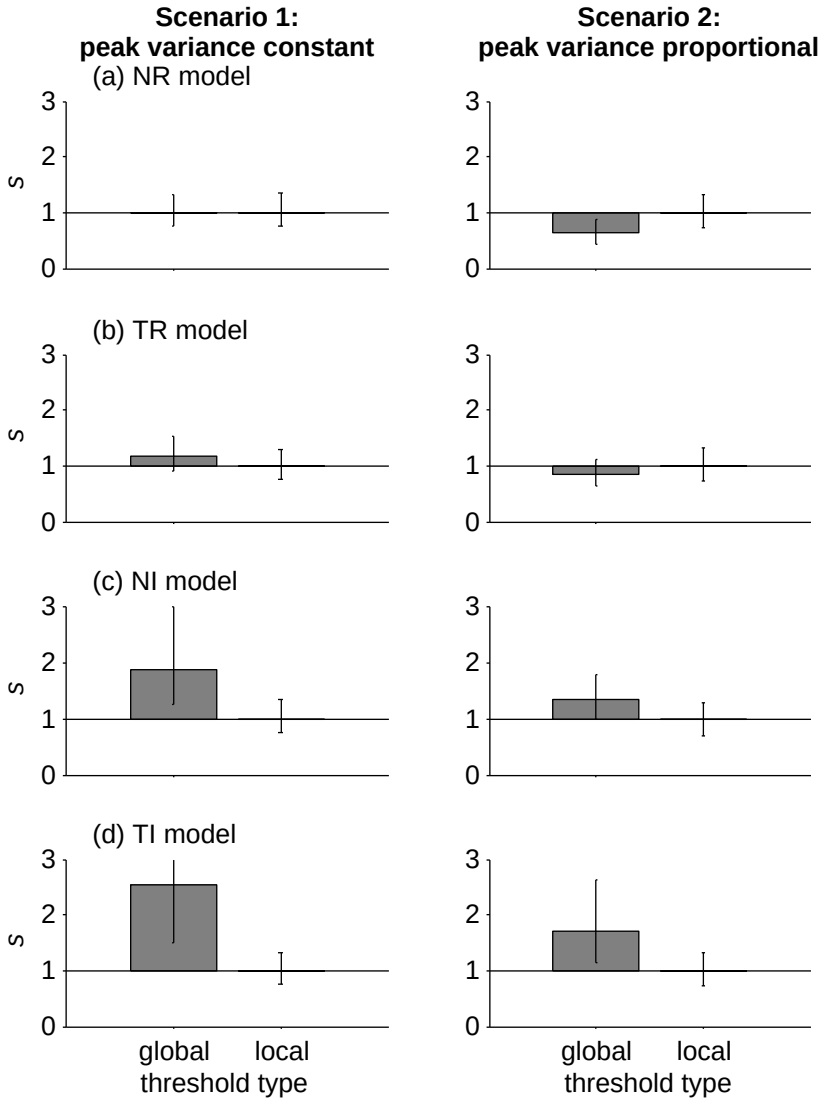
Scenario 1:
peak variance constant
Scenario 2:
peak variance proportional
(a) NR model
(b) TR model
(c) NI model
(d) TI model
s
0
1
2
3
global
local
threshold type

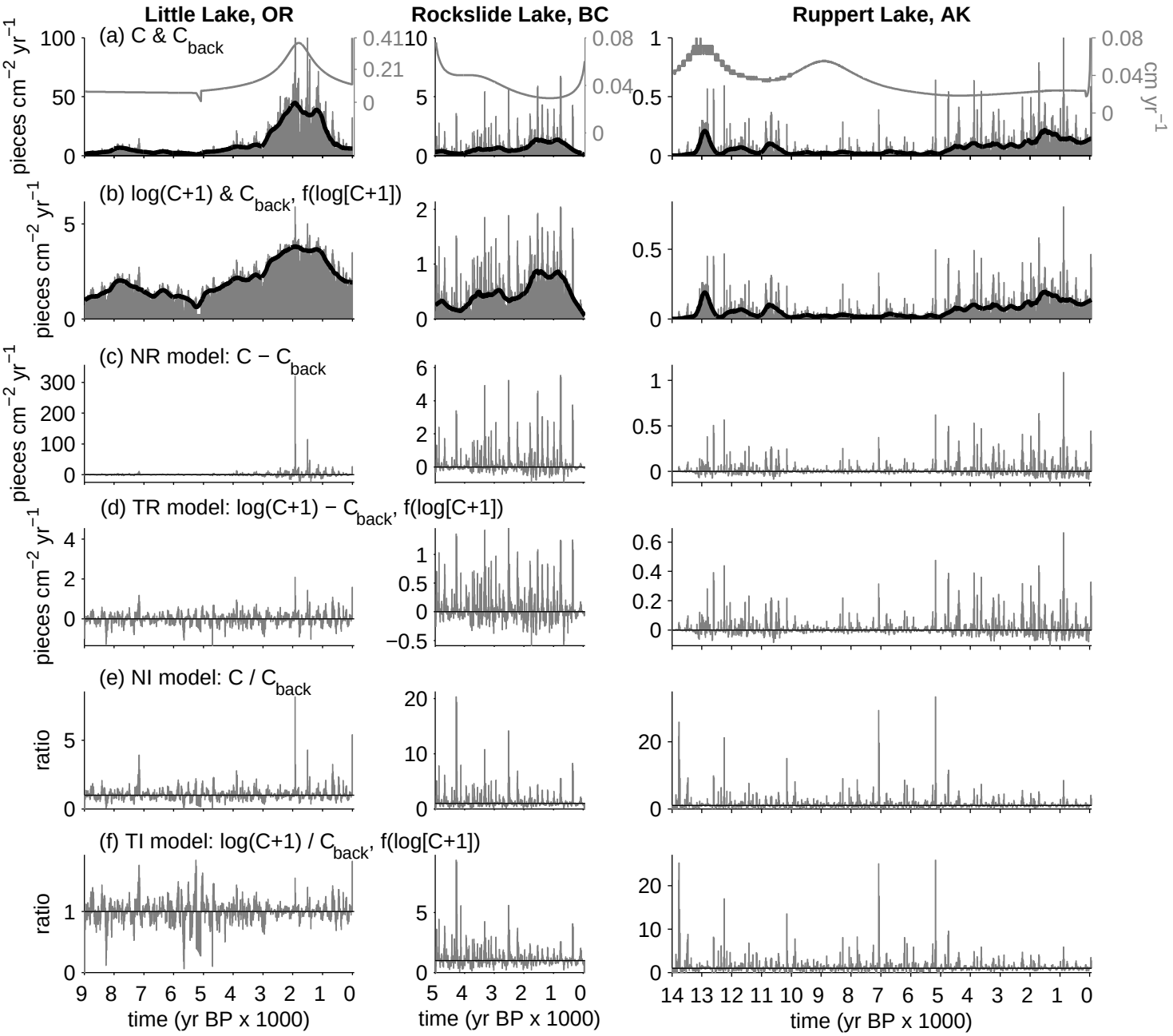
Little Lake, OR
Rockslide Lake, BC
Ruppert Lake, AK
(a) C & C back
(b) log(C+1) & C back, f(log[C+1])
(c) NR model: C − C back
(d) TR model: log(C+1) − C back, f(log[C+1])
(e) NI model: C / C back
(f) TI model: log(C+1) / C back, f(log[C+1])
pieces cm −2 yr −1
ratio
cm yr −1
time (yr BP x 1000)

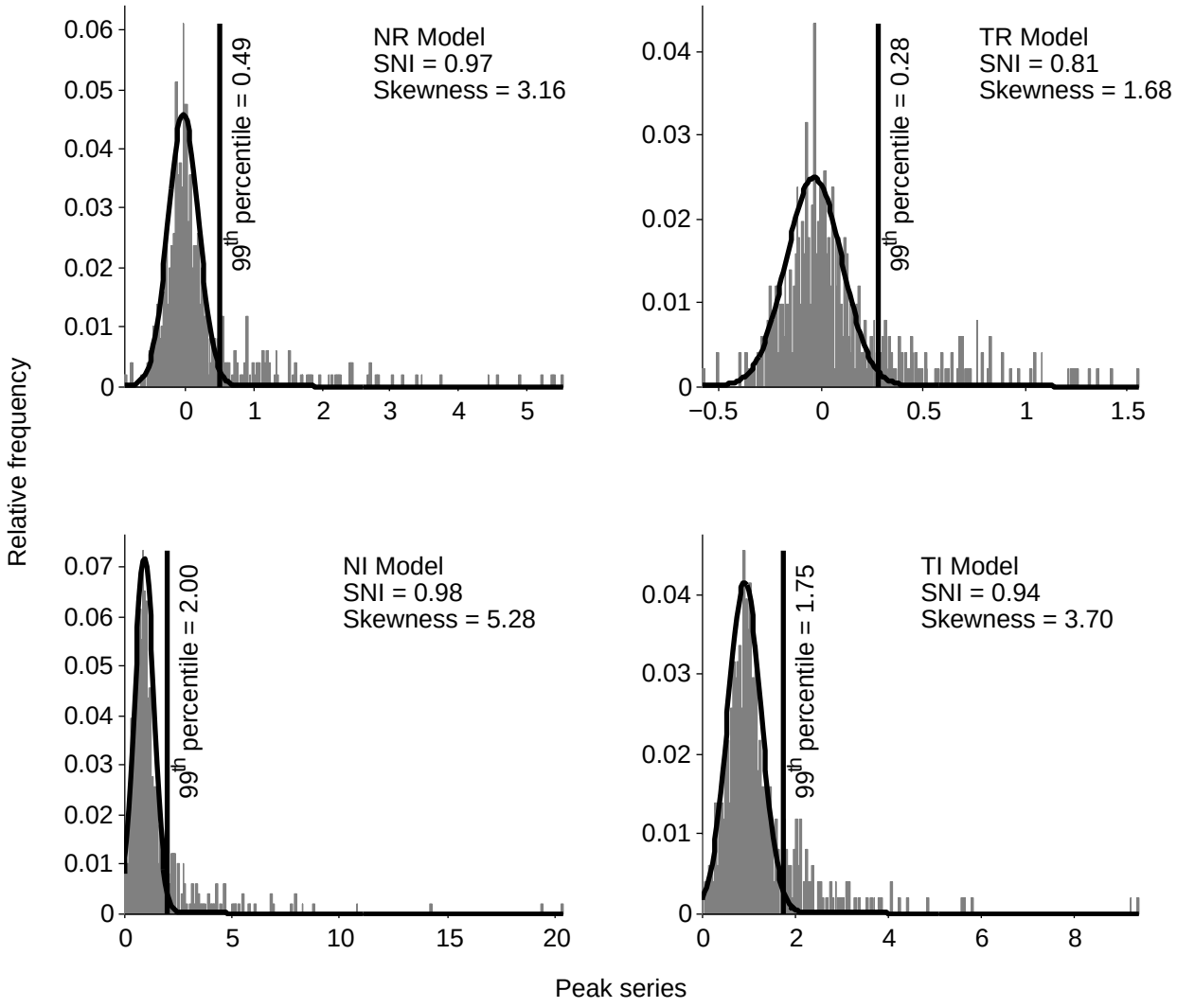
NR Model
SNI = 0.97
Skewness = 3.16
99th percentile = 0.49
TR Model
SNI = 0.81
Skewness = 1.68
99th percentile = 0.28
NI Model
SNI = 0.98
Skewness = 5.28
99th percentile = 2.00
TI Model
SNI = 0.94
Skewness = 3.70
99th percentile = 1.75
Relative frequency
Peak series

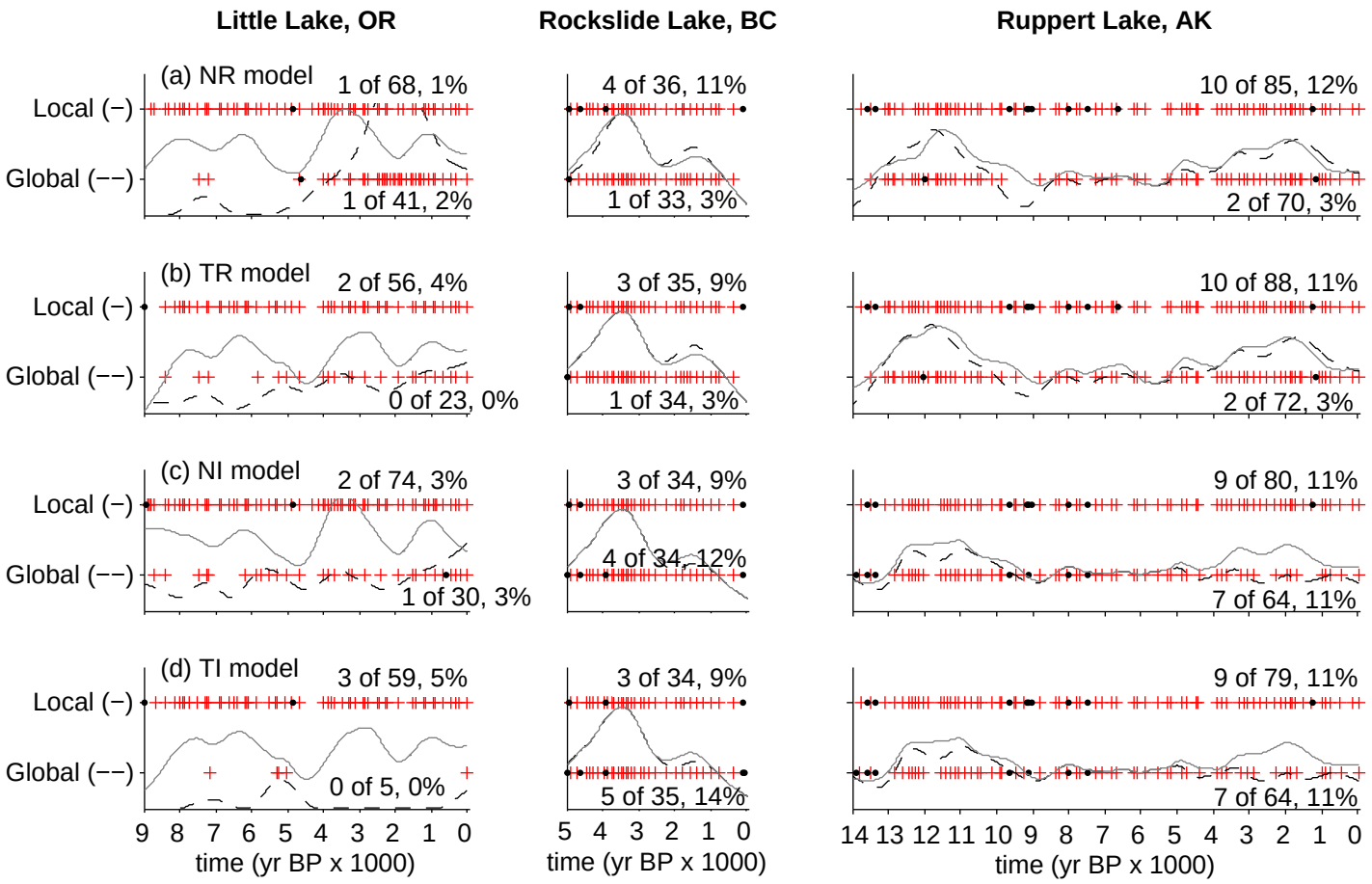
Little Lake, OR
Rockslide Lake, BC
Ruppert Lake, AK
(a) NR model
Local (−)
Global (−−)
1 of 68, 1%
1 of 41, 2%
4 of 36, 11%
1 of 33, 3%
10 of 85, 12%
2 of 70, 3%
(b) TR model
2 of 56, 4%
0 of 23, 0%
3 of 35, 9%
1 of 34, 3%
10 of 88, 11%
2 of 72, 3%
(c) NI model
2 of 74, 3%
1 of 30, 3%
3 of 34, 9%
4 of 34, 12%
9 of 80, 11%
7 of 64, 11%
(d) TI model
3 of 59, 5%
0 of 5, 0%
3 of 34, 9%
5 of 35, 14%
9 of 79, 11%
7 of 64, 11%
9 8 7 6 5 4 3 2 1 0
5 4 3 2 1 0
14 13 12 11 10 9 8 7 6 5 4 3 2 1 0
time (yr BP x 1000)
time (yr BP x 1000)
time (yr BP x 1000)

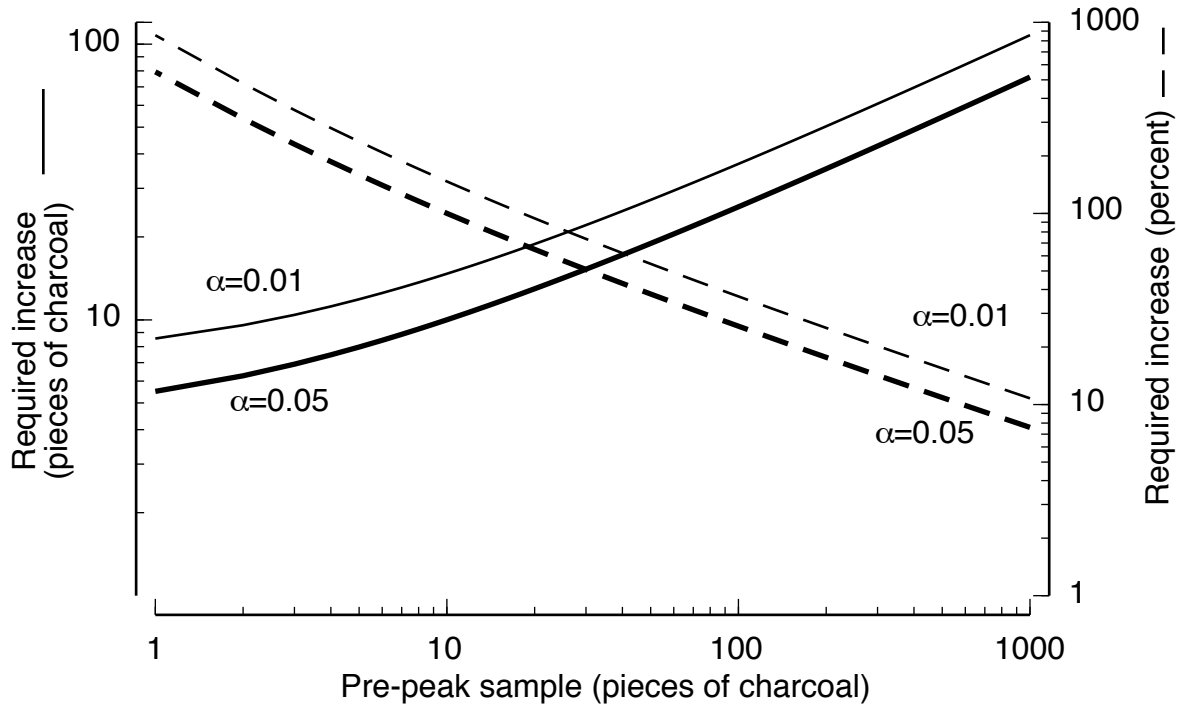
100
10
1000
100
10
1
Required increase
(pieces of charcoal)
Required increase (percent)
α=0.01
α=0.05
α=0.01
α=0.05
1
10
100
1000
Pre-peak sample (pieces of charcoal)